2001年12月よりbcr/ablに特異的に作用する新規薬剤が厚生労働省より異例の早さで承認された．これは，図6で示すように，Imatinib mesylate（Glivec）というチロシンキナーゼ阻害剤であり[9]，bcr/abl以外にもc-kitおよびPDGFRなどのチロシンキナーゼも阻害し，CML以外にも好酸球増加症候群などにも効果がみられ，また消化管間質腫瘍（GIST）にも使用されている．このImatinibは，欧米でのIRIS Study[10]でImatinib対IFN-α＋AraCのクロスオーバー試験がなされ，血液学的寛解率，細胞遺伝学的寛解率および薬剤耐容度においてImatinibの圧倒的有用性が確認された（図7）．

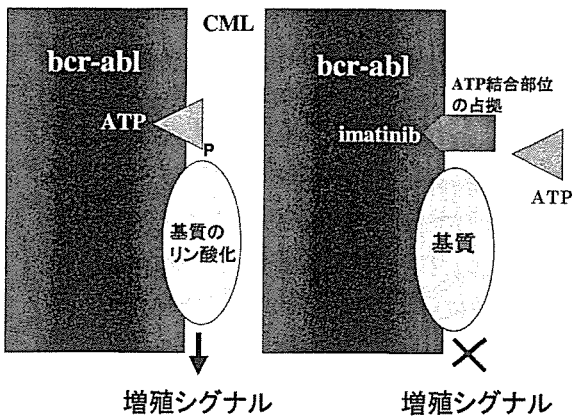

図6　imatinibの作用機序

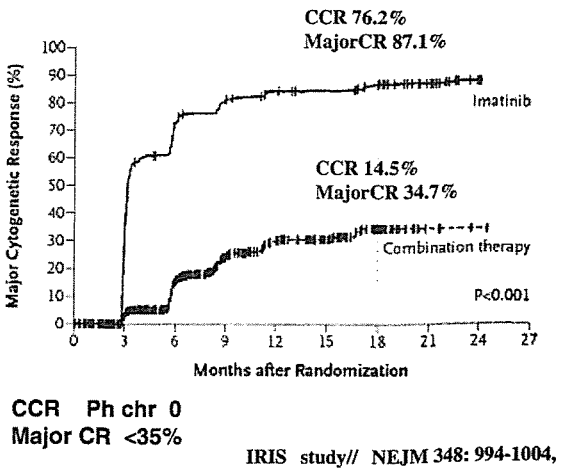

図7　Imatinib compared with interferon and low-dose cytarabine for newly diagnosed chronic-phase chronic myeloid ieukemia. Randomized trial of 1106 patients

最近5年間の長期成績も発表され細胞遺伝学的にPh染色体の消失は約90％にみられ，移行期や急性転化なく生存する率も90％以上と画期的な治療成績が得られた．この分子標的治療薬は，内服剤であり，アレルギー反応や軽度の肝障害，浮腫，嗄声などの副作用がみられるものの一時的減量・中止などの対応でほとんどの症例で長期投与が可能である．このことからImatinibはCML治療のfirst line therapyとして確固たる位置を築いた．問題点は，治療抵抗性を示す症例の存在が明らかとなりbcr/abl分子の遺伝子変異が出現しアミノ酸置換（Pループ内T315I）によりImatinibの結合が阻害されるメカニズムが解明されている[11]．このことから他の作用機序を有するチロシンキナーゼ阻害剤の開発が進められ，新たな治療戦略の中に組み込まれるのも近いと考えられる．

3．骨髄増殖性疾患の発症メカニズム

骨髄増殖性疾患（MPD）は，骨髄幹細胞レベルでの何らかの遺伝子異常に伴い骨髄3系統の増殖がみられる疾患群であり，主に赤血球が増加する真性赤血球増加症（PV），血小板が著増する本態性血小板血症（ET）ならびに骨髄が反応性に線維化する原発性骨髄線維症（MF）に分けられる．これらの疾患は，CMLと同様に細胞増殖は著明であるが，分化成熟障害はみられないのが特徴である．しかし，芽球の増加をきたす急性転化が高率にみられ，予後不良となることもCMLとよく似ている．臨床的観察からMPD発症機序もCMLと同様に細胞内チロシンキナーゼ活性の恒常的活性化をきたしていることが推測され，多くの細胞内増殖に関わる分子がスクリーニングされた結果，JAK2分子の変異が同定された．JAK2分子は，エリスロポエチン受容体，トロンボポエチン受容体ならびにG-CSF受容体などが，それぞれのリガンドと結合したとき2量体を形成し細胞内ドメインのチロシン残基がリン酸化されると，JAK2はこの受容体分子の細胞質内ドメインに会合し自己リン酸化されキナーゼ活性が亢進し，基質となるSTAT分子をリン酸化して，リン酸化STATが核内に移行し増殖に関わる遺伝子の上流に結合し転写を促し細胞増殖に導くことが知られている．MPD患者白血球に，このJAK2

分子の pseudokinase domain V617F の変異が発見された．Pseudokinase domain は C 末端に存在するキナーゼ活性を負に制御する機能を有しているが，V617F 変異によりこの負の制御がなくなり恒常的に JAK 2 シグナルが伝達されることにより細胞増殖を来すことが明らかになった（図 8）．JAK2変異は PV では 90 %以上の例でみられ，ET や MF でも 50 %程度にみられる．しかし，CML を含めた他の白血病ではみられない[12]．同じ JAK 2 変異により表現型が異なる疾患が発症することは説明ができず，未知の遺伝子異常が関与していることが推察される．当然のことながら MPD の分子標的治療薬としての JAK 2 キナーゼの特異的阻害剤の開発が待たれる．

4．造血幹細胞移植の新たな動き

一般的な化学療法で寛解に至らないか再発した難治性白血病では，同種造血幹細胞移植が行われる．これには同胞間あるいは骨髄バンクを介した非血縁者に HLA が一致したドナーの存在が必須である．よって，症例によってはドナー候補がいなくて移植ができないことも多々見られた．また，感染症や臓器障害のため同種移植を断念せざるを得ないことも多々みられる．このような移植適応制限を大きく広げることが可能となる移植術の開発も進められている．

移植細胞ソースとして，従来は骨髄幹細胞あるいは末梢血幹細胞に限られていたが，臍帯血の中にある幹細胞を利用する臍帯血移植（cord blood stem cell transplantation : CBT）が急激に増加してきた．全国に臍帯血バンクが設立され供給も問題なく行われるようになり，以前は小児に限られていたが，成人にも行われ非血縁者間骨髄移植数を上まわりつつある．CBT の最大のメリットは，HLA が 2 座不一致までは通常移植可能であり，移植片対宿主病（GVHD）もコントロール可能である．また，ドナーへの負担がなく，悪性細胞が急速増殖のため移植待機不可能時での緊急供給が可能である．しかし，CBT は臍帯血中の幹細胞数に限界があるため成人例では細胞数不足のこともあり，また生着までの期間が多少長くなることが問題点としてあげられる．現在 CBT の位置づけは各施設により異なるが，骨髄バンクでの HLA 一致非血縁者ドナーが不在の場合に行うことが多い．現在のところ臍帯血移植は，一定の成果が得られていることに加え，HLA の

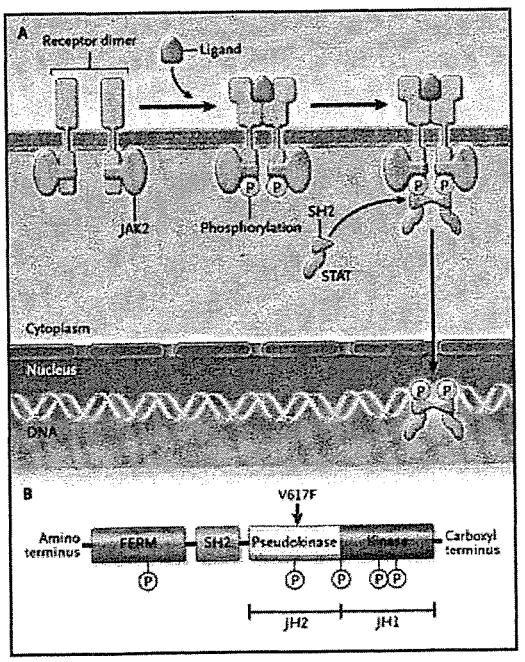

JAK2変異
骨髄増殖性疾患で高頻度でみられる。

JAK2
exon12
1849 G->T mutation
V617F

JH2 Pseudokinase domain

Levine RL, et al. Cancer cell 7; 387-397, 2005

図 8

しばりが拡がることにより移植可能症例数は，今後も増加することが予想されより良い臍帯血確保が社会的に必要となるであろう[12]．

従来の移植は，前処置として大量抗癌剤あるいは放射線照射によって骨髄を完全に破壊して造血免疫機構を回復不可能にし，さらに白血病細胞を根絶することにより，新たなドナー由来の幹細胞が生着することを可能にすることが必要であった．そのためレシピエントには，大きな負担を強いることになり，高齢者や臓器障害をもった患者への移植適応の限界があった．しかし，骨髄を完全に破壊しなくても免疫抑制を充分に行えばドナー由来の幹細胞の生着が得られ，自己複製能および血球細胞への分化成熟がみられることがヒトでも確認され骨髄非破壊的移植が行われるようになった[14]．骨髄非破壊的移植にも，前処置の強さにより，ほとんど骨髄抑制血球減少を来さないものから，かなり強い抗癌化学療法および放射線照射をくわえるレジメンまでいろいろあり，統一されたレジメンはない．しかし，免疫抑制（フルダラビン・ATGなど）は強力に行う必要がある．この方法により55歳までが限界であった同種移植も65歳まで可能であり，化学療法中の感染症合併例や心肺肝腎機能低下例なども適応になる．骨髄非破壊的移植は，前処置としての殺細胞効果は弱いことから，主たる抗白血病作用は移植ドナー由来Tリンパ球が残存しているレシピエントの白血病細胞を攻撃する移植片対白血病効果（GVL効果）といわれる免疫反応が主体となる．よって，残存白血病細胞が多い場合は，再発が多くなるため，移植前にはなるべく白血病細胞を減らしておく必要がある．

造血幹細胞移植も，適応年齢が拡がり，移植細胞ソースも増え，HLAの不適合移植例も増加しつつある現在，移植症例は飛躍的に増加することが予想される．これにより，難治性白血病の長期生存が期待できるようになるとともにその適応基準を明確にすることが今後求められるであろう．

ま と め

造血器腫瘍の病態解析は急速に進み，異常遺伝子，原因蛋白のレベルで論じられるようになった．これにより白血病の分類も従来の形態だけでなく分子論的な分類も取り入れられるようになり，治療反応性や予後についても均一な疾患分類が可能となり，この分類に基づいた治療法の選択が必要になりつつある．また，異常分子の同定に伴い，その特異的分子標的治療法の開発も急速に進行している．造血器腫瘍のみでなく他の悪性腫瘍にも応用が進み，将来の悪性腫瘍患者予後の改善に貢献できるものと期待する．

参 考 文 献

1）Jaffe ES, Harris NL, Stein H, Vardiman JW : Pathology and genetics. Tumours of haematopoietic and lymphoid tissues. World Health Organization Classification of Tumours. IARC Press Lyon, 2001

2）Grignani F et al : Fusion protein of the retinoic acid receptor alpha recruits histone deacetylase in promyelocytic leukemia. Nature, 391 : 815－818, 1998

3）Mistry AR et al : The molecular pathogenesis of acute promyelocytic leukaemia : implications for the clinical management of the disease. Blood rev, 17 : 71－97, 2003

4）Asou N et al : Analysis of prognostic factors in newly diagnosed patients with acute promyelocutic leukemia : the APL 92 study of the Japan Adult Leukemia Study Group (JALSG). Cancer Chemother Pharmacol, 48 : S65－S71, 2002

5）Nakao M et al : Internal tandem duplication of the flt3 gene found in acute myeloid leukemia. Keukemia, 10 : 1911－1918, 1996

6）Kiyoi H et al : Clinical significance of FLT3 in leukemia. Int J Hematol, 82 : 85－92, 2005

7）Falini B et al : Cytoplasmic nucleophosmin in acute nyelogenous leukemia with a normal karyotype. N Engl J Med, 352 : 254－266, 2005

8）Sattler M, Griffin JD : Molecular mechanisms of transformation by BCR-

ABL oncogene. Semin Hematol, **40** : 4 - 10, 2003

9) Druker BJ et al : Efficacy of a selective inhibitor of the Abl tyrosine kinase on the growth of BCR-ABL positive cells. Nat Med, **2** : 561 - 566, 1996

10) O ' Brien SG et al : Imatinib compared with interferon and low-dose cytarabine for newly diagnosed chronic-phase chronic myeloid leukemia. N Engl J Med, **348** : 994 - 1004, 2003

11) Gambacorti-Passerini C et al : Molecular mechanisms of resistance to imatinib in Philadelphia-chromosome-positive leukemias. Lancet Oncol, **4** : 75 - 85, 2003

12) Baxter EJ et al : Acquired mutation of the tyrosine kinase JAK 2 in human myeloproliferative disorders. Lancet, **365** : 1054 - 1061, 2005

13) Takahashi S et al : Single-institute comparative analysis of unrelated bone marrow transplantation and cord blood transplantation for adult patients with hematologic malignanies. Blood, **104** : 3813 - 3820, 2004

14) Slavin S et al : Nonmyeloablative stem cell transplantation and cell therapy as an alternative to conventional bone marrow transplantation with lethal cytoreduction for the treatment of malignant and nonmalignant hematologic diseases. Blood, **91** : 756 - 763, 1998

Therapeutic angiogenesis by ex vivo expanded erythroid progenitor cells

Shuji Sasaki,[1] Toyoshi Inoguchi,[1] Koichiro Muta,[1] Yasunobu Abe,[1] Min Zhang,[1] Kenichi Hiasa,[2] Kensuke Egashira,[2] Noriyuki Sonoda,[1] Kunihisa Kobayashi,[1] Ryoichi Takayanagi,[1] and Hajime Nawata[1]

[1]*Department of Medicine and Bioregulatory Science and* [2]*Department of Cardiovascular Medicine, Graduate School of Medical Sciences, Kyushu University, Fukuoka, Japan*

Submitted 31 March 2006; accepted in final form 17 September 2006

Sasaki S, Inoguchi T, Muta K, Abe Y, Zhang M, Hiasa K, Egashira K, Sonoda N, Kobayashi K, Takayanagi R, Nawata H. Therapeutic angiogenesis by ex vivo expanded erythroid progenitor cells. *Am J Physiol Heart Circ Physiol* 292: H657–H665, 2007. First published September 22, 2006; doi:10.1152/ajpheart.00343.2006.— Recent reports have demonstrated that erythroid progenitor cells contain and secrete various angiogenic cytokines. Here, the impact of erythroid colony-forming cell (ECFC) implantation on therapeutic angiogenesis was investigated in murine models of hindlimb ischemia. During the in vitro differentiation, vascular endothelial growth factor (VEGF) secretion by ECFCs was observed from *day 3* (burst-forming unit erythroid cells) to *day 10* (erythroblasts). ECFCs from *day 5* to *day 7* (colony-forming unit erythroid cells) showed the highest VEGF productivity, and *day 6* ECFCs were used for the experiments. ECFCs contained larger amounts of VEGF and fibroblast growth factor-2 (FGF-2) than peripheral blood mononuclear cells (PBMNCs). In tubule formation assays with human umbilical vein endothelial cells, ECFCs stimulated 1.5-fold more capillary growth than PBMNCs, and this effect was suppressed by antibodies against VEGF and FGF-2. Using an immunodeficient hindlimb ischemia model and laser-Doppler imaging, we evaluated the limb salvage rate and blood perfusion after intramuscular implantation of ECFCs. ECFC implantation increased both the salvage rate (38% vs. 0%, $P < 0.05$) and the blood perfusion (82.8% vs. 65.6%, $P < 0.01$). In addition, ECFCs implantation also significantly increased capillaries with recruitment of vascular smooth muscle cells and the capillary density was 1.6-fold higher than in the control group. Continuous production of human VEGF from ECFCs in the skeletal muscle was confirmed at least 7 days after the implantation. Implantation of ECFCs promoted angiogenesis in ischemic limbs by supplying angiogenic cytokines (VEGF and FGF-2), suggesting a possible novel strategy for therapeutic angiogenesis.

peripheral arterial disease; transplantation; ischemia

ALTERNATIVE THERAPIES for clinical limb ischemia have become very important for patients with peripheral arterial disease (PAD), who cannot undergo surgical or percutaneous revascularization. Pharmacological treatments have been shown to have no favorable effects on the natural history of critical limb ischemia (14). Delivery of angiogenic growth factors, such as vascular endothelial growth factor (VEGF) (13, 35, 38), fibroblast growth factor-2 (FGF-2) (3, 27), hepatocyte growth factor (22, 23), stromal cell-derived factor-1α (10, 39), and placental growth factor (18), using recombinant proteins or gene transfer has been considered for alternative treatment of PAD, and their efficacy has been demonstrated. However, angiogenesis is a well-harmonized process established by vascular network maturation and remodeling and involves the recruitment of mural cells (pericytes and smooth muscle cells) to the nascent endothelium. This process may be too complicated for effective stimulation by administration of a single angiogenic factor.

Endothelial progenitor cells (EPCs) have been shown to participate in postnatal neovascularization after mobilization from the bone marrow (1). Therapeutic induction of EPCs obtained from ex vivo expansion of peripheral blood (15), cord blood (24), or bone marrow (34) improved blood perfusion after ischemia and rescued ischemic limbs from autoamputation in animal models, although preparation of the large numbers of EPCs required for a therapeutic effect is difficult. Bone marrow mononuclear cells (BMMNCs) contain not only EPCs but also various potent angiogenic cytokines (16), and cell therapy for PAD using BMMNCs produced feasible angiogenic effects in experimental limb ischemia and clinical trials (36). On the other hand, implantation of peripheral blood mononuclear cells (PBMNCs) also showed effective induction of angiogenesis, although the implanted PBMNCs contained considerably fewer CD34-positive ($CD34^+$) cells than the BMMNCs (0.02% vs. 2.4%) (11). These results may provide the concept that the effect of PBMNCs or BMMNCs is mainly derived from the supply of angiogenic factors rather than the involvement of EPCs.

Recent reports have demonstrated that burst-forming unit erythroid (BFU-E) progenitor cells express high levels of VEGF mRNA (19, 29) and that erythroblasts secrete VEGF and placental growth factor proteins during in vitro differentiation (37). Although these results suggest an important role for erythroid progenitor cells in angiogenesis, no studies have reported in vivo evidence of angiogenesis induction by erythroid progenitor cells.

In the present study, we investigated the angiogenic potential of peripheral blood-derived erythroid colony-forming cells (ECFCs) and evaluated whether implantation of ECFCs could represent a novel angiogenic cell therapy.

METHODS

Reagents. Recombinant human erythropoietin (rhEPO) was kindly provided by Chugai Pharmaceutical (Tokyo, Japan), whereas recombinant human interleukin-3 and recombinant human stem cell factor (rhSCF) were kindly provided by Kirin-Brewery (Tokyo, Japan). Neutralizing antibodies against VEGF, FGF-2, and transforming growth factor-β (TGF-β) were purchased from R&D Systems (Minneapolis, MN), and a mouse anti-rat CD31 antibody was obtained from BD Biosciences (San Diego, CA). A mouse anti-α-smooth muscle actin (SMA) antibody and the 5-bromo-4-chloro-3-indolyl phosphate/nitro blue tetrazolium (BCIP/NBT) color substrates were purchased from Sigma (St. Louis, MO). Fluorescent carbocyanine 1,1′-dioctadecyl-1 to

Address for reprint requests and other correspondence: T. Inoguchi, Dept. of Medicine and Bioregulatory Science, Graduate School of Medical Sciences, Kyushu Univ., 3-1-1 Maidashi, Higashi-ku, Fukuoka 812-8582, Japan (e-mail: toyoshi@intmed3.med.kyushu-u.ac.jp).

The costs of publication of this article were defrayed in part by the payment of page charges. The article must therefore be hereby marked "*advertisement*" in accordance with 18 U.S.C. Section 1734 solely to indicate this fact.

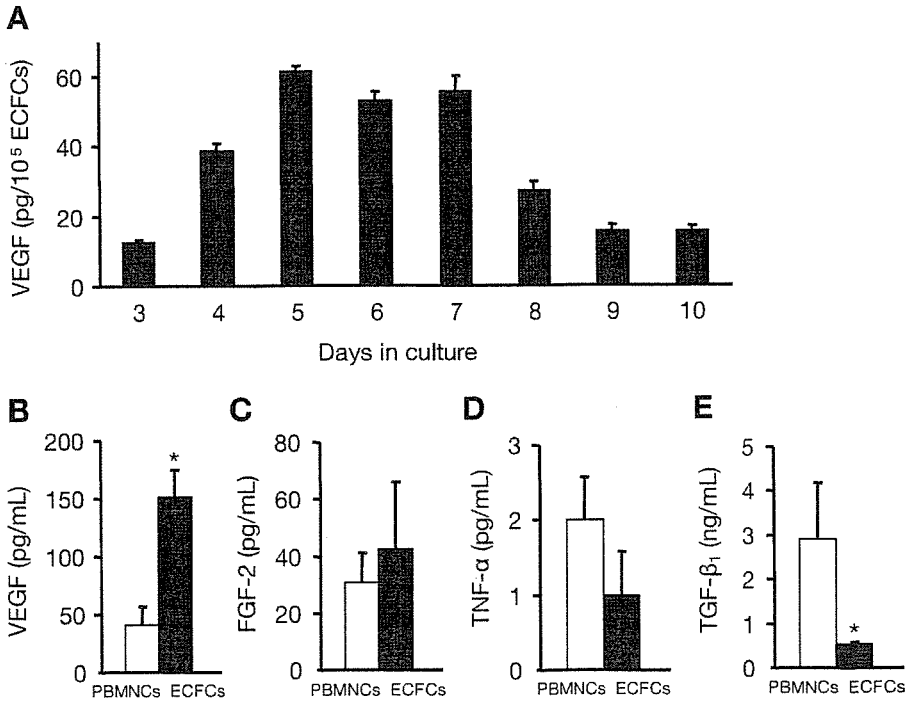

Fig. 1. Angiogenic cytokines in erythroid colony-forming cells (ECFCs). *A*: vascular endothelial growth factor (VEGF) secretion from ECFCs during in vitro differentiation. *Day 3* ECFCs correspond to burst-forming unit erythroid (BFU-E) progenitor cells, *day 5* to *day 7* ECFCs correspond to colony-forming unit erythroid (CFU-E) progenitor cells, and *day 10* ECFCs correspond to erythroblasts (n = 3 for each). *B–E*: intracellular levels of angiogenic cytokines in *day 6* ECFCs and peripheral blood mononuclear cells (PBMNCs). *B*: VEGF; *C*: fibroblast growth factor-2 (FGF-2); *D*: tumor necrosis factor-α (TNF-α); *E*: transforming growth factor-β (TGF-β). Cellular extracts were obtained from ECFCs (1×10^7) and PBMNCs (1×10^7) by freezing and thawing, and the concentrations of the different cytokines in the cellular extracts were measured by ELISA (n = 3 for each). $^*P < 0.05$.

3,3,3′3′-tetramethylindocarbocyanine perchlorate dye was purchased from Molecular Probes (Eugene, OR).

Preparation of ECFCs and PBMNCs. ECFCs were prepared as previously described (31, 32). Briefly, light density mononuclear cells were isolated from heparinized peripheral blood buffy coats (70 ml) from healthy Japanese volunteers by density centrifugation through lymphocyte separation medium (density 1.0770–1.0800 g/ml: ICN Biomedicals, Aurora, OH). Red blood cells were lysed by suspending the mononuclear cell pellet in red blood cell lysis buffer (0.16 mol/l ammonium chloride, 10 mmol/l potassium bicarbonate, and 5 mmol/l EDTA). Platelets were removed by centrifugation in phosphate-buffered saline (PBS) containing 10% human serum albumin (kindly provided by the Chemo-Sero-Therapeutic Research Institute, Kumamoto, Japan). At this point, the cells were collected and used as PBMNCs in experiments. Adherent cells were depleted by 1-h incubation in a polystyrene tissue culture flask at 4°C. Nonadherent cells were collected, and negative selection was performed using antibodies against CD3, CD11b, CD15, and CD45RA and immunomagnetic beads in Vario-Macs columns (Miltenyi Biotech, Auburn, CA). The remaining cells were cultured in Iscove's modified Dulbecco's medium (IMDM; GIBCO-BRL, Grand Island, NY) containing 15% heat-inactivated fetal calf serum (FCS: Commonwealth Serum, Melbourne, VIC, Australia), 15% pooled human serum, 2 U/ml EPO, 20 ng/ml SCF, and 10 ng/ml IL-3 at 37°C in 5% CO_2-95% air in a high-humidity incubator (*day 0*). On *day 3*, the cells (referred to as *day 3* ECFCs) were centrifuged through lymphocyte separation medium and collected and incubated under the same conditions, except for the absence of SCF. ECFCs were collected on *day 3* to *day 10* and used in experiments. Homogeneous expression of cell surface markers for erythroid maturation, glycophorin A and transferrin receptor, were confirmed as previously described by us (21). The morphological purity of the *day 6* ECFCs was 95 ± 3%, as determined by cytospin preparations.

Enzyme-linked immunosorbent assays. VEGF production by ECFCs was detected using a Quantikine Immunoassay kit (R&D Systems) according to the manufacturer's instructions. The intracellular levels of VEGF, FGF-2, tumor necrosis factor-α (TNF-α), and TGF-β in *day 6* ECFCs and PBMNCs were detected using specific immunoassays for human VEGF (R&D Systems), FGF-2 (R&D Systems), TNF-α (Japan Immunoresearch, Takasaki, Japan), and TGF-β (Otsuka Pharmaceutical, Tokyo, Japan) according to each manufacturer's instructions.

Endothelial tubule formation. Tubule formation experiments were conducted in triplicate using an Angiogenesis kit (Kurabo, Osaka, Japan), according to the manufacturer's instructions as previously reported (6, 17, 40). Briefly, human umbilical vein endothelial cells (HUVECs) and human fibroblasts were admixed and seeded into 24-well plates. For experiments, various numbers of ECFCs were cocultured with HUVECs using cell culture inserts (BD, Bedford, MA) settled in the wells of the plates. Medium containing 2% FCS was supplemented every 3 days. After 10 days of culture, the HUVECs were fixed with 70% ethanol at 4°C and immunostained with an anti-human CD31 antibody using BCIP/NBT as the substrate for the secondary antibody. Five fields per well were selected for digital photography under a microscope (Olympus, Tokyo, Japan), and the areas of the tubule-like structures were measured quantitatively using an angiogenesis image analyzer software (Kurabo) (28, 40). Neutralizing antibodies against VEGF, FGF-2, TNF-α, or TGF-β were preincubated with cell-conditioned medium for 60 min, as described previously (11).

An animal model of hindlimb ischemia and transplantation of ECFCs. This study was approved by the Committee on the Ethics of Animal Experiments, Graduate School of Medical Sciences, Kyushu University (Fukuoka, Japan). Hindlimb ischemia was created by resecting the left femoral arteries and veins (7) of immunodeficient nude mice (BALB/c nu/nu; Charles River Japan, Yokohama, Japan) as "an autoamputation model" or nude rats (F344/N rnu/rnu; CLEA Japan, Tokyo, Japan) as "a limb salvage model" under anesthesia with pentobarbital sodium (50 mg/kg ip). All arterial branches were obliterated by ligation or electrocoagulation. ECFCs or PBMNCs (1×10^6 cells in 50 μl IMDM for mice; 1×10^7 cells in 200 μl IMDM for rats) were implanted intramuscularly into the ischemic thigh area (divided into 4 sites) followed by injection of 1,000 IU/kg rhEPO to protect the ECFCs from apoptosis. For the control groups, the same volume of PBS with or without 1,000 IU/kg EPO was injected into the ischemic thigh area.

Limb salvage rate and laser-Doppler analysis. In the autoamputation model, the hindlimbs were photographed at 2 wk after the operation, and the appearances were classified visually into the following three grades: *1*) complete salvage (completely normal status

with no signs of ischemia); *2*) limb necrosis (necrosis of tissue below the knee); and *3*) autoamputation (necrosis of tissue above the knee or loss of the limb), as described previously (15).

In the limb salvage model, a laser-Doppler perfusion imager (Moor Instruments, Devon, UK) was used to measure blood flow in the ischemic and nonischemic limbs.

Immunohistochemistry. Ischemic tissues from the thigh muscles of rats in the limb salvage model were obtained at 4 wk after the operation. Frozen sections (10-μm thickness) were subjected to mouse anti-rat CD31 antibody staining to show the capillary morphology and alkaline phosphatase (ALP) staining by the indoxyl-tetrazolium method to reveal the biochemical activity of the vascular endothelial cells (7, 41). Digital images of 20 fields from two sections were randomly selected from each animal for capillary counts.

Serum concentration of VEGF and FGF-2. Blood samples were collected from rats at postoperative *days 0, 1, 3* and *7*. After centrifugation, serum samples were subjected to ELISA using Quantikine Immunoassay Systems for human and mouse VEGFs and FGF-2 (R&D Systems) according to the manufacturer's instructions.

Intramuscular content of VEGF. Ischemic thigh muscles obtained from mice at postoperative *days 1, 4,* and *7* were minced and homogenized in 1 ml of PBS buffer containing protease inhibitors (Roche Diagnostics, Mannheim, Germany) on ice. After centrifugation, VEGF levels in the supernatants were determined using Quantikine Immunoassay Systems for human VEGF (R&D Systems). Levels of VEGF were expressed according to the muscle weight.

Statistical analysis. The results were expressed as means ± SE. Differences between two groups were analyzed using Student's *t*-test. Multiple comparisons among the groups were carried out by one-way ANOVA followed by Bonferroni's method. The incidence of limb salvage was evaluated by χ^2-analysis among the three groups. Data were considered significant at $P < 0.05$.

RESULTS

Angiogenic potential of ECFCs. During the in vitro differentiation, VEGF secretion from ECFCs was observed from *day 3* (corresponding to BFU-E progenitor cells) to *day 10*

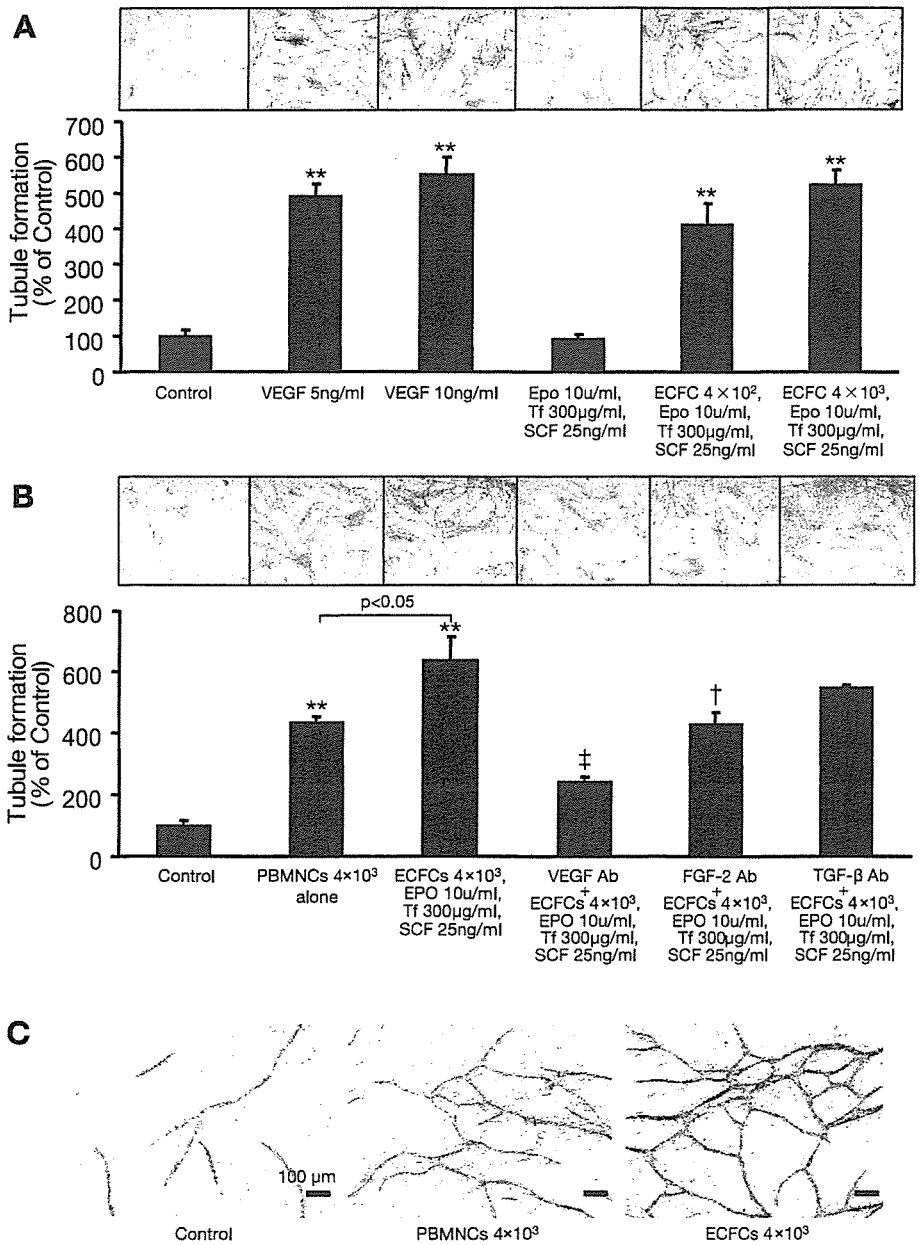

Fig. 2. Effect of ECFCs on endothelial tubule formation. Human umbilical vein endothelial cells (HUVECs) were cocultured with ECFCs or PBMNCs and then immunostained for CD31. *A*: tubule formation induced by various numbers of ECFCs (4×10^2 and 4×10^3). VEGF (5 and 10 ng/ml) samples were used as positive controls. *B*: comparison of the tubule formation induced by ECFCs (4×10^3) and PBMNCs (4×10^3) and the effects of neutralizing antibodies against VEGF, FGF-2, and TGF-β on tubule formation. *C*: higher-power images of the culture assays in *B*. Bar, 100 μm. Tf, transferrin; EPO, erythropoietin; SCF, stem cell factor. $^{**}P < 0.01$ vs. control; $^{\dagger}P < 0.05$ and $^{\ddagger}P < 0.01$ vs. ECFCs.

(corresponding to erythroblasts). As shown in Fig. 1*A*, ECFCs from *days 5* to *7* [corresponding to colony-forming unit erythroid (CFU-E) progenitor cells] possessed the highest VEGF productivity. Therefore, *day 6* ECFCs were used in the following experiments. ECFCs also contained various angiogenic factors, such as FGF-2, TNF-α, and TGF-β, in addition to VEGF. The intracellular levels of angiogenic cytokines in *day 6* ECFCs were compared with those in PBMNCs. The VEGF content was 3.7-fold higher in ECFCs than in PBMNCs (Fig. 1*B*; 151.7 vs. 41.0 pg/ml, $P < 0.05$). The FGF-2 level was also higher (Fig. 1*C*; 42.7 vs. 30.7 pg/ml), although the statistical significance was marginal. The TGF-β level was significantly lower in ECFCs than in PBMNCs (Fig. 1*E*; 0.51 vs. 2.91 ng/ml, $P < 0.05$).

ECFCs surpass PBMNCs for stimulation of tubule formation. In the tubule formation assays, HUVEC were immunostained with an anti-CD31 antibody, and the colored areas were quantified as capillary growth. After coculture for 8 days, the capillary tubule formation induced by ECFCs (4×10^3 cells) was 5.2-fold greater than that induced by medium containing 2% FCS (Fig. 2*A*). A similar magnitude of tubule formation was induced by 10 ng/ml VEGF. EPO, transferrin, and SCF without ECFCs did not significantly affect the tubule formation. Furthermore, the tubule formation induced by ECFCs was 1.5-fold greater than that induced by PBMNCs, and this effect was significantly suppressed by supplementation with antibodies against VEGF (Fig. 2*B*; 62.3% suppression, $P < 0.01$) and FGF-2 (Fig. 2*B*; 32.9% suppression, $P < 0.05$).

Intramuscular ECFC implantation salvages ischemic limbs from autoamputation. In the autoamputation model using athymic nude mice, the mice develop extensive necrosis or autoamputation of the ischemic hindlimb. We classified the mice according to the degree of ischemia at 2 wk after the operation as shown in Fig. 3. More than one-half of the mice (54%) injected with PBS developed autoamputation, and none of the mice (0%) exhibited complete salvage. As for PBMNC-implanted mice, only 31% exhibited autoamputation, but none of the mice exhibited complete salvage. In contrast, 38% of mice implanted with ECFCs exhibited successful complete salvage, and only 31% developed autoamputation. Statistical analysis revealed a significantly higher rate of complete limb salvage in the ECFC group than in the PBS group or PBMNC group (38% vs. 0%, $P < 0.05$).

Enhanced blood perfusion in ischemic limbs implanted with ECFCs. To investigate blood perfusion in the hindlimbs after implantation of ECFCs, we used athymic nude rats. None of these model rats developed extensive necrosis or autoamputation of the ischemic hindlimb. The rats were implanted with ECFCs (1×10^7 cells) followed by EPO (1,000 IU/kg), EPO (1,000 IU/kg) alone or PBS. At 4 days after the operation, limb blood perfusion was severely reduced in all three groups. At 14 days after the operation, significant enhancement of the blood perfusion was observed in the ECFC group compared with the PBS group. (Fig. 4, *A* and *B*; 82.88% vs. 54.16%, $P < 0.05$). Finally, at 28 days after the operation, the ECFC group showed significantly augmented blood perfusion compared with the EPO (82.82% vs. 70.57%, $P < 0.05$) and PBS (82.82% vs. 65.55%, $P < 0.01$) groups. No significant differences were observed between the EPO and PBS groups.

Serum concentrations of angiogenic cytokines. We measured the serum levels of human VEGF and FGF-2 in the ECFC and PBS groups. Systemic concentrations of human VEGF and FGF-2 were undetectable at *days 1*, *3*, or *7* (data not shown).

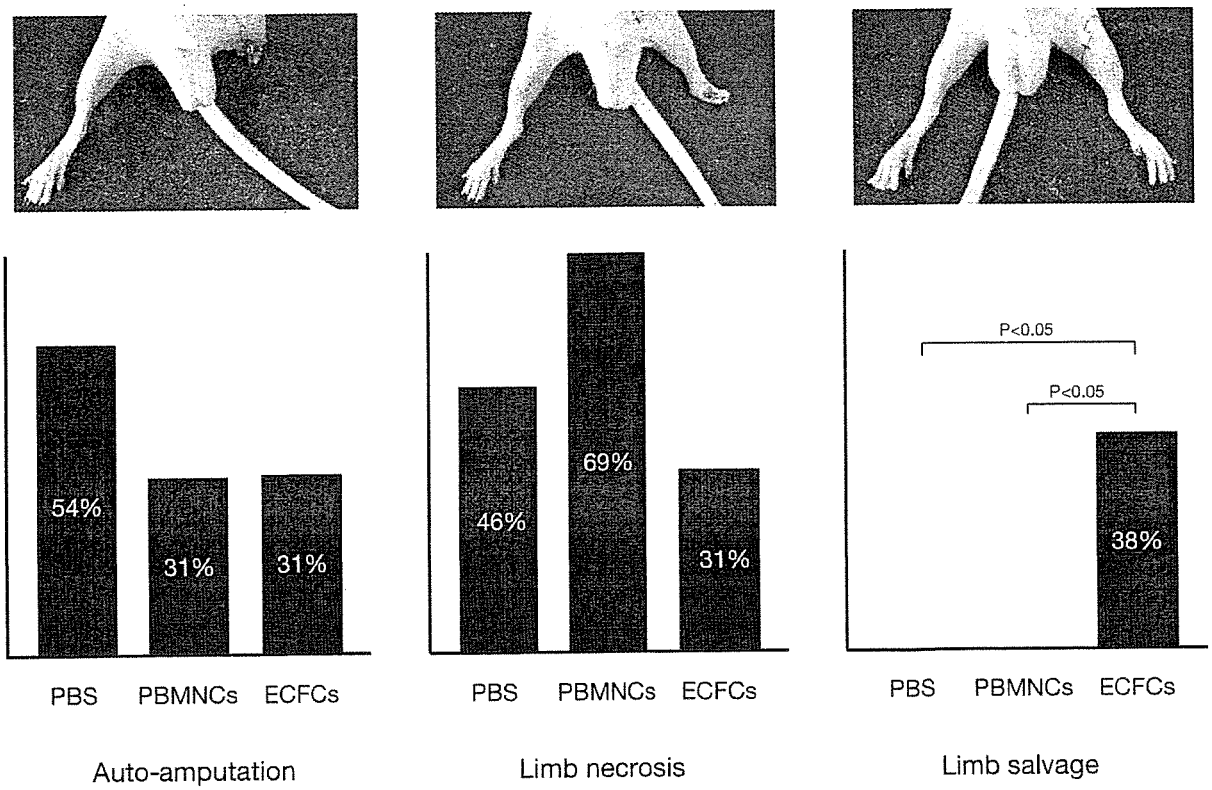

Fig. 3. Limb outcomes at 2 wk after the operation in an autoamputation model. Representative macroscopic photographs showing the three different grades classified by the degree of ischemia. Percent distributions of the outcomes were evaluated by χ^2-analysis among mice receiving ECFCs ($n = 16$), PBMNCs ($n = 13$), and PBS ($n = 13$). The incidence of limb salvage was statistically significant.

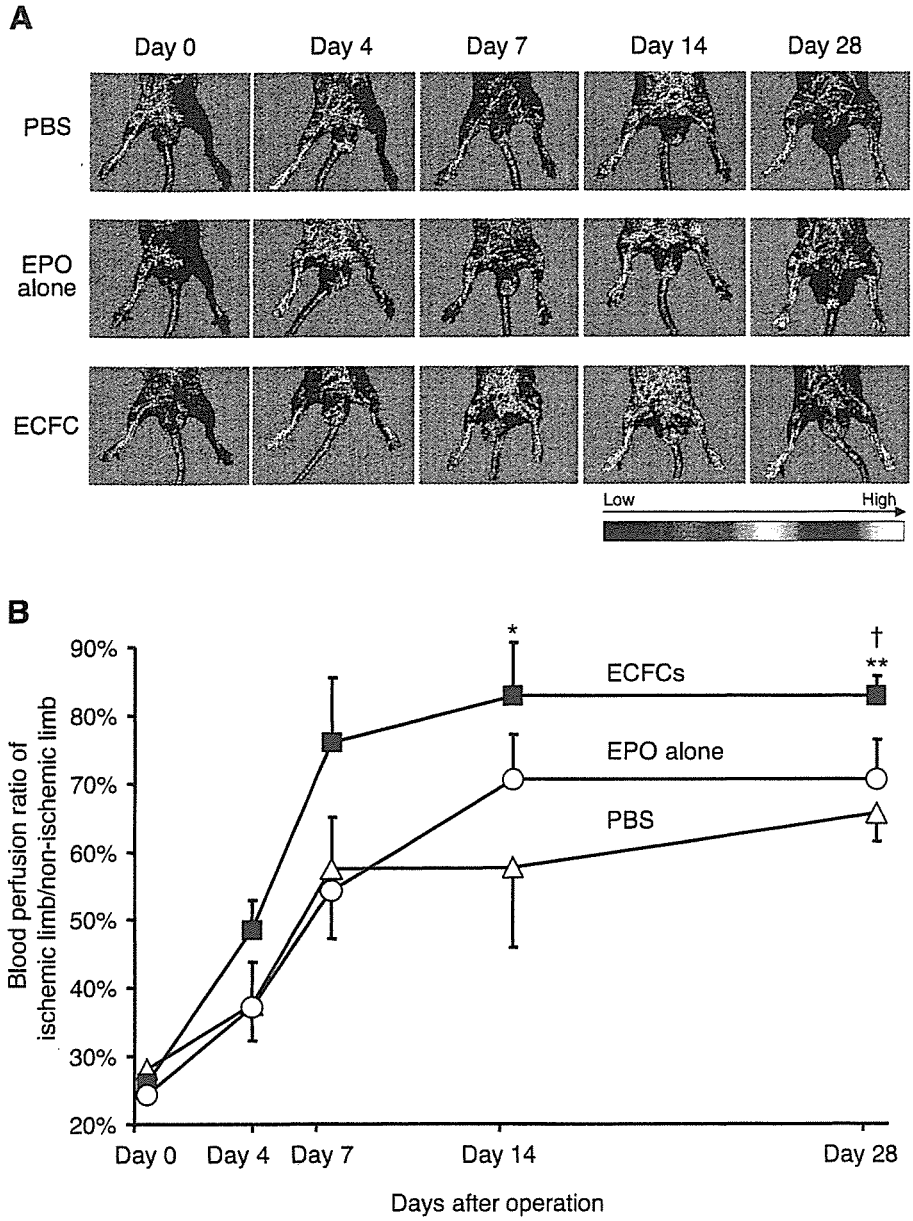

Fig. 4. Laser-Doppler perfusion image analysis of the ECFC group (n = 11), EPO-alone group (n = 10), and PBS group (n = 7). *A*: representative digital color-coded images indicating the blood flow distributions over the time course. *B*: blood perfusion represented by the blood perfusion ratios of the ischemic limb to the nonischemic limb. $^{*}P < 0.05$ and $^{**}P < 0.01$ vs. PBS; $\dagger P < 0.01$ vs. EPO alone.

Intramuscular content of angiogenic cytokines. We measured the levels of human VEGF in the ischemic hindlimbs of the ECFC and PBS groups (Fig. 5). The implanted ECFCs produced human VEGF after the intramuscular implantation. The human VEGF content in homogenized muscle was abundant at *day 1* after the implantation (515.4 pg/g muscle). Human VEGF production lasted up to 7 days after the implantation.

Increased capillary density confirms ECFC-induced angiogenesis. To confirm new capillary formation microscopically, we stained frozen sections of ischemic hindlimbs obtained at 28 days after the operation, using three different approaches. Briefly, anti-CD31 staining was used to define the morphology, ALP staining was used to assess the vascular endothelial bioactivity, and anti-α-SMA staining was used to confirm the stability and maturity of vessels (Fig. 6*A*). According to the anti-CD31 staining, the capillary density was 1.6-fold higher in the ECFC group than in the EPO and PBS groups (Fig. 6*B*) (389.0/mm^2 vs. 265.3/mm^2 and 255.9/mm^2, respectively, $P <$ 0.01 for each). No significant differences were observed between the EPO and PBS groups. Significant differences were also found in both the ALP staining and anti-α-SMA staining between the ECFC group and the EPO and PBS groups (ALP: 209.8/mm^2 vs. 137.8/mm^2 and 132.4/mm^2, respectively, $P <$ 0.01 for each; anti-α-SMA: 179.8/mm^2 vs. 115.8/mm^2 and 106.9/mm^2, respectively, $P < 0.05$ for each).

DISCUSSION

Various angiogenic factors and cytokines induce angiogenesis and vasculogenesis by collaborative interactions, but the detailed molecular mechanism is not fully understood. VEGF is acknowledged to play a key role in this process and is generally considered to be the most important modulator. It induces the formation of collateral vessels and increases collateral blood flow, leading to improvement in endothelium-dependent vasodilation (5). In addition, it also directly upregu-

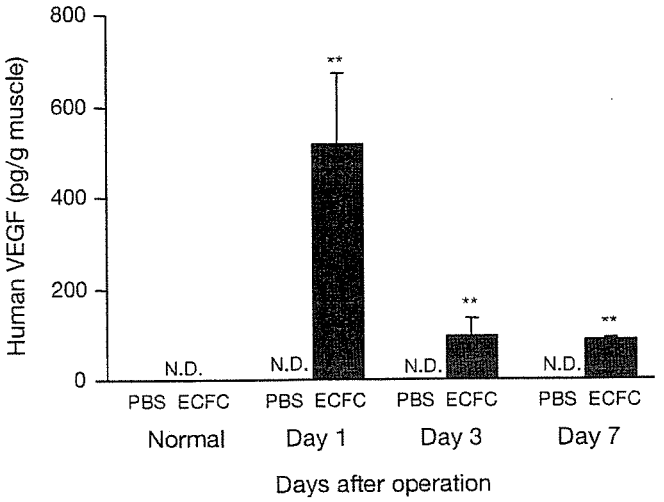

Fig. 5. Intramuscular content of human VEGF. ECFC-implanted or PBS-injected muscles (n = 6 for each) were obtained from mice at postoperative *days 1*, *4*, and *7*, and the VEGF content in the homogenized muscles was evaluated by ELISA. The values were expressed as means ± SE; ND, not detected. $^{**}P < 0.01$ vs. PBS.

lates endothelial nitric oxide synthase expression, consequently increasing nitric oxide release (33). However, transgenic or adenoviral overexpression of VEGF resulted in the formation of vessels that were hyperpermeable and leaky. Masaki et al. (20) reported that overexpressed VEGF in ischemic muscle may be insufficient to induce maturation of the capillaries and that the concerted actions of FGF-2 and VEGF may be necessary for functional mature neovascularization accompanied by a smooth muscle cell lining. These results suggest that combinations of various angiogenic factors may be required for functional mature neovascularization.

Recently, cell therapy for PAD using BMMNCs has produced feasible angiogenic effects in experimental limb ischemia and clinical studies (34, 36). BMMNCs contain not only various potent angiogenic cytokines but also EPCs. Circulating EPCs have been discovered in adult peripheral blood as well as human umbilical cord blood and are considered to differentiate into endothelial cells and participate in neovascularization after mobilization from the bone marrow (1). In fact, efficacy of EPC implantation has been demonstrated in experimental limb ischemia and patients with severe ischemia of the lower limbs (12, 15). On the other hand, PBMNC implantation was also reported to show effective induction of angiogenesis via the supply of angiogenic factors, although the implanted PBMNCs contained considerably fewer $CD34^+$ cells than the BMMNCs (0.02% vs. 2.4%) (11). This finding raised the possibility that the supply of angiogenic factors can induce functional mature angiogenesis without the supply of EPCs.

Previously, it has been shown that BFU-E progenitor cells express a high level of VEGF mRNA (19, 29) and that erythroblasts secrete VEGF and placental growth factor proteins during in vitro differentiation (37). In the present study, we revealed that peripheral blood-derived ECFCs produced VEGF during in vitro differentiation from BFU-E progenitor cells to erythroblasts, whereas CFU-E progenitor cells showed the highest VEGF productivity. ECFCs also showed abundant production of FGF-2, in addition to VEGF. These results suggest that erythroid progenitor cells may have an important role in angiogenesis and also suggest the possibility of novel therapeutic angiogenesis using erythroid progenitor cells. The current study represents the first investigation of whether ex vivo-expanded peripheral blood-derived ECFCs can augment functional angiogenesis in both in vitro and in vivo models of critical limb ischemia. The results revealed that *1*) ECFCs stimulated capillary tubule formation in coculture assays with HUVECs, mainly by supplying VEGF and FGF-2; *2*) intramuscular implantation of ECFCs significantly increased the limb salvage rate in an autoamputation model using athymic nude mice; *3*) intramuscular implantation of ECFCs significantly increased blood perfusion in a limb salvage model using athymic nude rats; *4*) capillary density increased in rats implanted with ECFCs; *5*) not only vascular endothelial cells but vascular smooth muscle cells were increased in ECFC-implanted muscle; and *6*) the implanted cells survived and produced VEGF up to 7 days after implantation. These results demonstrate that ECFC implantation augmented functional angiogenesis with recruitment of vascular smooth muscle cells in critical limb ischemia via the cooperative supply of angiogenic factors, especially VEGF and FGF-2. However, it remained to be evaluated whether ECFCs acted only as a cytokine donor. In addition, elevated cytokines might induce the mobilization or homing of circulating EPCs (2). The detailed mechanism requires further investigation.

Given its efficacy, implantation of ECFCs appears to have several advantages. First, implantation of autologous ECFCs does not induce toxicity or immunologic rejection compared with methods involving human recombinant proteins, naked plasmid DNAs or viruses. Second, ECFCs can easily be obtained from the peripheral blood and expanded ex vivo. The collection of mononuclear cells or EPCs from the bone marrow requires general anesthesia, while more than 5–6 liters of peripheral blood are needed to obtain a sufficient number of mononuclear cells that are rich in EPCs (39). In the present study, immature erythroid progenitor cells were partially purified from peripheral blood by negative selection with antibodies against CD3, CD11b, CD15, and CD45RA and then differentiated into mature erythroid progenitor cells in the presence of EPO, SCF, and IL-3. During this ex vivo culture, immature progenitor cells at *day 3* were finally expanded to almost 15-fold mature progenitor cells at *day 6*. With the use of this culture system, large-scale ex vivo amplification for clinical use can be performed to obtain a sufficient number of erythroid progenitor cells (8). Third, the ECFCs we used were not pluripotent, and cell lineage was committed only to erythroid. Thus ECFC implantation appears to be very safe since they finally differentiate into erythrocytes.

In the present study, we coadministered EPO (1,000 U/kg) to protect the cells from apoptosis since a previous study revealed that 70% of ECFCs underwent apoptosis within 16 h in serum-free liquid culture without EPO, compared with only 23% in the presence of EPO (25). EPO is known to be involved in the cell viability and proliferation of ECFCs (26). Recent reports have suggested an angiogenic effect of EPO. EPO stimulated the proliferation and migration of cultured HUVECs (30), promoted EPC mobilization from the bone marrow (4, 9), and increased blood perfusion in ischemic limbs. In contrast with these reports, EPO alone had no significant effect on capillary tubule formation and did not significantly augment blood perfusion in the ischemic hindlimb

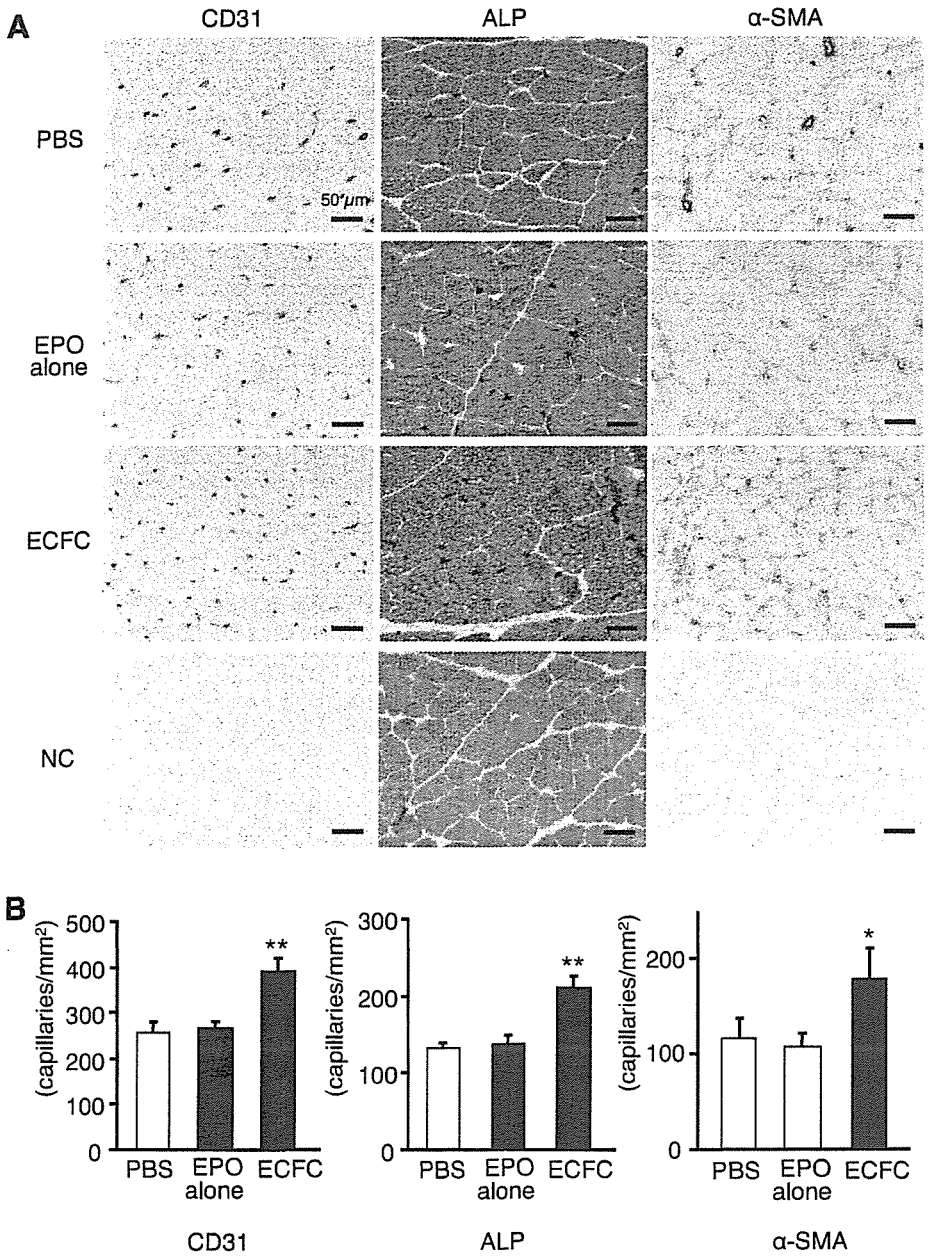

Fig. 6. Immunohistochemical analysis of capillary formation. Capillary formation was evaluated by anti-CD31 staining for the morphology (*left*), ALP staining for the vascular endothelial bioactivity (*middle*), and anti-α-smooth muscle actin (SMA) staining for the vascular maturity (*right*). *A*: digital images of 20 microscopic fields from 2 sections were obtained from each animal for capillary counts: PBS group ($n = 5$), EPO-alone group ($n = 5$), and ECFC group ($n = 4$). NC, negative control; ALP, alkaline phosphatase. *B*: quantitative analysis of the capillary density. $^{*}P < 0.05$ and $^{**}P < 0.01$ vs. PBS. Bar, 50 μm.

model in the present study. However, it remained possible that EPO promoted EPC mobilization from the bone marrow and augmented ECFC-induced neovascularization. Future studies are needed to address the effects of EPO on in vivo angiogenesis.

In summary, we demonstrated for the first time that intramuscular implantation of peripheral blood-derived ECFCs into ischemic limbs effectively induced functional collateral vessel formation with recruitment of vascular smooth muscle cells via the supply of various angiogenic factors, especially VEGF and FGF-2. ECFCs can easily be obtained from patients, even those with complications of ischemic heart disease, diabetes, or other severe arteriosclerosis and who have a high risk for general anesthesia. This novel angiogenic cell therapy appears to be feasible, although its clinical efficacy should be tested in human trial.

ACKNOWLEDGMENTS

We thank Dr. T. Murohara of the Department of Cardiology, Nagoya University Graduate School of Medicine for excellent comments and advice.

REFERENCES

1. **Asahara T, Murohara T, Sullivan A, Silver M, van der Zee R, Li T, Witzenbichler B, Schatteman G, Isner JM.** Isolation of putative progenitor endothelial cells for angiogenesis. *Science* 275: 964–967, 1997.
2. **Asahara T, Takahashi T, Masuda H, Kalka C, Chen D, Iwaguro H, Inai Y, Silver M, Isner JM.** VEGF contributes to postnatal neovascularization by mobilizing bone marrow-derived endothelial progenitor cells. *EMBO J* 18: 3964–3972, 1999.
3. **Baffour R, Berman J, Garb JL, Rhee SW, Kaufman J, Friedmann P.** Enhanced angiogenesis and growth of collaterals by in vivo administration of recombinant basic fibroblast growth factor in a rabbit model of acute lower limb ischemia: dose-response effect of basic fibroblast growth factor. *J Vasc Surg* 16: 181–191, 1992.

4. **Bahlmann FH, De Groot K, Spandau JM, Landry AL, Hertel B, Duckert T, Boehm SM, Menne J, Haller H, Fliser D.** Erythropoietin regulates endothelial progenitor cells. *Blood* 103: 921–926, 2004.
5. **Bauters C, Asahara T, Zheng LP, Takeshita S, Bunting S, Ferrara N, Symes JF, Isner JM.** Recovery of disturbed endothelium-dependent flow in the collateral-perfused rabbit ischemic hindlimb after administration of vascular endothelial growth factor. *Circulation* 91: 2802–2809, 1995.
6. **Bishop ET, Bell GT, Bloor S, Broom IJ, Hendry NF, Wheatley DN.** An in vitro model of angiogenesis: basic features. *Angiogenesis* 3: 335–344, 1999.
7. **Couffinhal T, Silver M, Zheng LP, Kearney M, Witzenbichler B, Isner JM.** Mouse model of angiogenesis. *Am J Pathol* 152: 1667–1679, 1998.
8. **Giarratana MC, Kobari L, Lapillonne H, Chalmers D, Kiger L, Cynober T, Marden MC, Wajcman H, Douay L.** Ex vivo generation of fully mature human red blood cells from hematopoietic stem cells. *Nat Biotechnol* 23: 69–74, 2005.
9. **Heeschen C, Aicher A, Lehmann R, Fichtlscherer S, Vasa M, Urbich C, Mildner-Rihm C, Martin H, Zeiher AM, Dimmeler S.** Erythropoietin is a potent physiologic stimulus for endothelial progenitor cell mobilization. *Blood* 102: 1340–1346, 2003.
10. **Hiasa K, Ishibashi M, Ohtani K, Inoue S, Zhao Q, Kitamoto S, Sata M, Ichiki T, Takeshita A, Egashira K.** Gene transfer of stromal cell-derived factor-1alpha enhances ischemic vasculogenesis and angiogenesis via vascular endothelial growth factor/endothelial nitric oxide synthase-related pathway: next-generation chemokine therapy for therapeutic neovascularization. *Circulation* 109: 2454–2461, 2004.
11. **Iba O, Matsubara H, Nozawa Y, Fujiyama S, Amano K, Mori Y, Kojima H, Iwasaka T.** Angiogenesis by implantation of peripheral blood mononuclear cells and platelets into ischemic limbs. *Circulation* 106: 2019–2025, 2002.
12. **Inaba S, Egashira K, Komori K.** Peripheral-blood or bone-marrow mononuclear cells for therapeutic angiogenesis? *Lancet* 360: 2083; author reply 2084, 2002.
13. **Isner JM, Pieczek A, Schainfeld R, Blair R, Haley L, Asahara T, Rosenfield K, Razvi S, Walsh K, Symes JF.** Clinical evidence of angiogenesis after arterial gene transfer of phVEGF165 in patient with ischaemic limb. *Lancet* 348: 370–374, 1996.
14. **Isner JM, Rosenfield K.** Redefining the treatment of peripheral artery disease. Role of percutaneous revascularization. *Circulation* 88: 1534–1557, 1993.
15. **Kalka C, Masuda H, Takahashi T, Kalka-Moll WM, Silver M, Kearney M, Li T, Isner JM, Asahara T.** Transplantation of ex vivo expanded endothelial progenitor cells for therapeutic neovascularization. *Proc Natl Acad Sci USA* 97: 3422–3427, 2000.
16. **Kamihata H, Matsubara H, Nishiue T, Fujiyama S, Tsutsumi Y, Ozono R, Masaki H, Mori Y, Iba O, Tateishi E, Kosaki A, Shintani S, Murohara T, Imaizumi T, Iwasaka T.** Implantation of bone marrow mononuclear cells into ischemic myocardium enhances collateral perfusion and regional function via side supply of angioblasts, angiogenic ligands, and cytokines. *Circulation* 104: 1046–1052, 2001.
17. **Kiba A, Yabana N, Shibuya M.** A set of loop-1 and -3 structures in the novel vascular endothelial growth factor (VEGF) family member, VEGF-ENZ-7, is essential for the activation of VEGFR-2 signaling. *J Biol Chem* 278: 13453–13461, 2003.
18. **Luttun A, Tjwa M, Moons L, Wu Y, Angelillo-Scherrer A, Liao F, Nagy JA, Hooper A, Priller J, De Klerck B, Compernolle V, Daci E, Bohlen P, Dewerchin M, Herbert JM, Fava R, Matthys P, Carmeliet G, Collen D, Dvorak HF, Hicklin DJ, Carmeliet P.** Revascularization of ischemic tissues by PlGF treatment, and inhibition of tumor angiogenesis, arthritis and atherosclerosis by anti-Flt1. *Nat Med* 8: 831–840, 2002.
19. **Majka M, Janowska-Wieczorek A, Ratajczak J, Ehrenman K, Pietrzkowski Z, Kowalska MA, Gewirtz AM, Emerson SG, Ratajczak MZ.** Numerous growth factors, cytokines, and chemokines are secreted by human CD34$^-$ cells, myeloblasts, erythroblasts, and megakaryoblasts and regulate normal hematopoiesis in an autocrine/paracrine manner. *Blood* 97: 3075–3085, 2001.
20. **Masaki I, Yonemitsu Y, Yamashita A, Sata S, Tanii M, Komori K, Nakagawa K, Hou X, Nagai Y, Hasegawa M, Sugimachi K, Sueishi K.** Angiogenic gene therapy for experimental critical limb ischemia: acceleration of limb loss by overexpression of vascular endothelial growth factor 165 but not of fibroblast growth factor-2. *Circ Res* 90: 966–973, 2002.
21. **Matsushima T, Nakashima M, Oshima K, Abe Y, Nishimura J, Nawata H, Watanabe T, Muta K.** Receptor binding cancer antigen expressed on SiSo cells, a novel regulator of apoptosis of erythroid progenitor cells. *Blood* 98: 313–321, 2001.
22. **Morishita R, Aoki M, Hashiya N, Makino H, Yamasaki K, Azuma J, Sawa Y, Matsuda H, Kaneda Y, Ogihara T.** Safety evaluation of clinical gene therapy using hepatocyte growth factor to treat peripheral arterial disease. *Hypertension* 44: 203–209, 2004.
23. **Morishita R, Nakamura S, Hayashi S, Taniyama Y, Moriguchi A, Nagano T, Taiji M, Noguchi H, Takeshita S, Matsumoto K, Nakamura T, Higaki J, Ogihara T.** Therapeutic angiogenesis induced by human recombinant hepatocyte growth factor in rabbit hind limb ischemia model as cytokine supplement therapy. *Hypertension* 33: 1379–1384, 1999.
24. **Murohara T, Ikeda H, Duan J, Shintani S, Sasaki K, Eguchi H, Onitsuka I, Matsui K, Imaizumi T.** Transplanted cord blood-derived endothelial precursor cells augment postnatal neovascularization. *J Clin Invest* 105: 1527–1536, 2000.
25. **Muta K, Krantz SB.** Apoptosis of human erythroid colony-forming cells is decreased by stem cell factor and insulin-like growth factor I as well as erythropoietin. *J Cell Physiol* 156: 264–271, 1993.
26. **Muta K, Krantz SB, Bondurant MC, Wickrema A.** Distinct roles of erythropoietin, insulin-like growth factor I, and stem cell factor in the development of erythroid progenitor cells. *J Clin Invest* 94: 34–43, 1994.
27. **Ohara N, Koyama H, Miyata T, Hamada H, Miyatake SI, Akimoto M, Shigematsu H.** Adenovirus-mediated ex vivo gene transfer of basic fibroblast growth factor promotes collateral development in a rabbit model of hind limb ischemia. *Gene Ther* 8: 837–845, 2001.
28. **Oike Y, Ito Y, Maekawa H, Morisada T, Kubota Y, Akao M, Urano T, Yasunaga K, Suda T.** Angiopoietin-related growth factor (AGF) promotes angiogenesis. *Blood* 103: 3760–3765, 2004.
29. **Pomyje J, Zivny J, Sefc L, Plasilova M, Pytlik R, Necas E.** Expression of genes regulating angiogenesis in human circulating hematopoietic cord blood CD34$^+$/CD133$^+$ cells. *Eur J Haematol* 70: 143–150, 2003.
30. **Ribatti D, Presta M, Vacca A, Ria R, Giuliani R, Dell'Era P, Nico B, Roncali L, Dammacco F.** Human erythropoietin induces a pro-angiogenic phenotype in cultured endothelial cells and stimulates neovascularization in vivo. *Blood* 93: 2627–2636, 1999.
31. **Sawada K, Krantz SB, Dessypris EN, Koury ST, Sawyer ST.** Human colony-forming units-erythroid do not require accessory cells, but do require direct interaction with insulin-like growth factor I and/or insulin for erythroid development. *J Clin Invest* 83: 1701–1709, 1989.
32. **Sawada K, Krantz SB, Kans JS, Dessypris EN, Sawyer S, Glick AD, Civin CI.** Purification of human erythroid colony-forming units and demonstration of specific binding of erythropoietin. *J Clin Invest* 80: 357–366, 1987.
33. **Shen BQ, Lee DY, Zioncheck TF.** Vascular endothelial growth factor governs endothelial nitric-oxide synthase expression via a KDR/Flk-1 receptor and a protein kinase C signaling pathway. *J Biol Chem* 274: 33057–33063, 1999.
34. **Shintani S, Murohara T, Ikeda H, Ueno T, Sasaki K, Duan J, Imaizumi T.** Augmentation of postnatal neovascularization with autologous bone marrow transplantation. *Circulation* 103: 897–903, 2001.
35. **Takeshita S, Zheng LP, Brogi E, Kearney M, Pu LQ, Bunting S, Ferrara N, Symes JF, Isner JM.** Therapeutic angiogenesis. A single intraarterial bolus of vascular endothelial growth factor augments revascularization in a rabbit ischemic hind limb model. *J Clin Invest* 93: 662–670, 1994.
36. **Tateishi-Yuyama E, Matsubara H, Murohara T, Ikeda U, Shintani S, Masaki H, Amano K, Kishimoto Y, Yoshimoto K, Akashi H, Shimada K, Iwasaka T, Imaizumi T.** Therapeutic angiogenesis for patients with limb ischaemia by autologous transplantation of bone-marrow cells: a pilot study and a randomised controlled trial. *Lancet* 360: 427–435, 2002.
37. **Tordjman R, Delaire S, Plouet J, Ting S, Gaulard P, Fichelson S, Romeo PH, Lemarchandel V.** Erythroblasts are a source of angiogenic factors. *Blood* 97: 1968–1974, 2001.
38. **Tsurumi Y, Takeshita S, Chen D, Kearney M, Rossow ST, Passeri J, Horowitz JR, Symes JF, Isner JM.** Direct intramuscular gene transfer of naked DNA encoding vascular endothelial growth factor augments collateral development and tissue perfusion. *Circulation* 94: 3281–3290, 1996.
39. **Yamaguchi J, Kusano KF, Masuo O, Kawamoto A, Silver M, Murasawa S, Bosch-Marce M, Masuda H, Losordo DW, Isner JM,**

Asahara T. Stromal cell-derived factor-1 effects on ex vivo expanded endothelial progenitor cell recruitment for ischemic neovascularization. *Circulation* 107: 1322–1328, 2003.

40. **Yoshida T, Ohno-Matsui K, Ichinose S, Sato T, Iwata N, Saido TC, Hisatomi T, Mochizuki M, Morita I.** The potential role of amyloid beta in the pathogenesis of age-related macular degeneration. *J Clin Invest* 115: 2793–2800, 2005.
41. **Ziada AM, Hudlicka O, Tyler KR, Wright AJ.** The effect of long-term vasodilatation on capillary growth and performance in rabbit heart and skeletal muscle. *Cardiovasc Res* 18: 724–732, 1984.

THE JOURNAL OF BIOLOGICAL CHEMISTRY VOL. 282, NO. 10, pp. 7329–7338, March 9, 2007

Insulin-like Growth Factor 1/Insulin Signaling Activates Androgen Signaling through Direct Interactions of Foxo1 with Androgen Receptor*[S]

Received for publication, November 9, 2006, and in revised form, December 15, 2006 Published, JBC Papers in Press, January 2, 2007, DOI 10.1074/jbc.M610447200

WuQiang Fan[‡], Toshihiko Yanase[‡1], Hidetaka Morinaga[‡], Taijiro Okabe[‡], Masatoshi Nomura[‡], Hiroaki Daitoku[§], Akiyoshi Fukamizu[§], Shigeaki Kato[¶], Ryoichi Takayanagi[‡], and Hajime Nawata[‖]

From the [‡]Department of Medicine and Bioregulatory Science, Graduate School of Medical Science, Kyushu University, Maidashi 3-1-1, Higashi-ku, Fukuoka 812-8582, [§]Center for Tsukuba Advanced Research Alliance, Graduate School of Life and Environmental Sciences, University of Tsukuba, Tsukuba, Ibaraki 305-8577, [¶]Institute of Molecular and Cellular Biosciences, Graduate School of Agricultural and Life Sciences, University of Tokyo, Tokyo 113-0032, and [‖]Graduate School of Medical Science, Kyushu University, Maidashi 3-1-1, Higashi-ku, Fukuoka 812-8582, Japan

The androgen-androgen receptor (AR) system plays vital roles in a wide array of biological processes, including prostate cancer development and progression. Several growth factors, such as insulin-like growth factor 1 (IGF1), can induce AR activation, whereas insulin resistance and hyperinsulinemia are correlated with an elevated incidence of prostate cancer. Here we report that Foxo1, a downstream molecule that becomes phosphorylated and inactivated by phosphatidylinositol 3-kinase/Akt kinase in response to IGF1 or insulin, suppresses ligand-mediated AR transactivation. Foxo1 reduces androgen-induced AR target gene expressions and suppresses the *in vitro* growth of prostate cancer cells. These inhibitory effects of Foxo1 are attenuated by IGF1 but are enhanced when it is rendered Akt-nonphosphorylatable. Foxo1 interacts directly with the C terminus of AR in a ligand-dependent manner and disrupts ligand-induced AR subnuclear compartmentalization. Foxo1 is recruited by liganded AR to the chromatin of AR target gene promoters, where it interferes with AR-DNA interactions. IGF1 or insulin abolish the Foxo1 occupancy of these promoters. Of interest, a positive feedback circuit working locally in an autocrine/intracrine manner may exist, because liganded AR up-regulates IGF1 receptor expression in prostate cancer cells, presumably resulting in higher IGF1 signaling tension and further enhancing the functions of the receptor itself. Thus, Foxo1 is a novel corepressor for AR, and IGF1/insulin signaling may confer stimulatory effects on AR by attenuating Foxo1 inhibition. These results highlight the potential involvement of metabolic syndrome and hyperinsulinemia in prostate diseases and further suggest that intervention of IGF1/insulin-phosphatidylinositol 3-kinase-Akt signaling may be of clinical value for prostate diseases.

Androgen receptor (AR)[2] is a member of a nuclear receptor superfamily and functions as a ligand-dependent transcription factor. The androgen-AR system mediates male sexual differentiation in the uterus, sperm production at puberty, prostate development in the adult, and primary prostate cancer (PC) growth in patients with PC (1). PC is the most common malignancy in men worldwide and the second leading cause of cancer-related mortality in the United States (2). The fact that over 70% of PCs rely on androgen stimulation for growth sets the basis for androgen ablation therapy, which is initially effective but invariably results in treatment resistance after a period of time (3). The disease is then referred to as androgen-independent PC and progresses to a fatal outcome. Recent loss-of-function studies have revealed that AR still plays a key role in hormone-refractory progression of PC (4, 5). An adaptation of AR signaling in order to function under low or absent androgen levels may occur (6). Among the various suggested mechanisms by which AR may be reactivated in a low androgen environment (7), signaling by growth factors, especially insulin-like growth factor 1 (IGF1), is reportedly of significant importance (8–11). High IGF1 serum levels are correlated with an increased risk of PC (8, 9), whereas IGF1 enhances AR transactivation under very low or absent androgen levels (12, 13) and promotes PC cell proliferation (10). Recent studies have also revealed that high serum insulin levels are associated with an increased incidence of PC (14, 15), although there is a lack of mechanistic studies implicating insulin signaling in the regulation of AR function.

Foxo1, also known as FKHR, together with other two homologs, FKHRL1 and AFX, belong to the Foxo subfamily of the forkhead transcription factor family, which includes a large array of transcription factors characterized by the presence of a

* This work was supported by a grant-in-aid for the "Mechanism of Sex Differentiation" and a grant from the 21st Century COE Program from the Ministry of Education, Culture, Sports, Science, and Technology of Japan. The costs of publication of this article were defrayed in part by the payment of page charges. This article must therefore be hereby marked "*advertisement*" in accordance with 18 U.S.C. Section 1734 solely to indicate this fact.

[S] The on-line version of this article (available at http://www.jbc.org) contains supplemental Figs. 1–9.

[1] To whom correspondence should be addressed. Tel.: 81-92-642-5280; Fax: 81-92-642-5287; E-mail: yanase@intmed3.med.kyushu-u.ac.jp.

[2] The abbreviations used are: AR, androgen receptor; hAR, human AR; ARE, androgen-response element; ChIP, chromatin immunoprecipitation; DHT, 5α-dihydrotestosterone; ER, estrogen receptor; GAPDH, glyceraldehyde-3-phosphate dehydrogenase; GR, glucocorticoid receptor; IGF1, insulin-like growth factor 1; IGF1R, insulin-like growth factor 1 receptor; MMTV, mouse mammary tumor virus; PC, prostate cancer; PI3K, phosphatidylinositol 3-kinase; PR, progesterone receptor; PSA, prostate-specific antigen; PTEN, human phosphatase and tensin homolog (mutated in multiple advanced cancers 1; EIA, enzyme immunoassay; PBS, phosphate-buffered saline; ANOVA, analysis of variance; HI, heterogeneity index.

conserved 110-amino acid winged helix DNA-binding domain (16). Foxo subfamily members play important roles in cell cycle regulation and apoptosis, as well as in metabolic homeostasis (17).

Phosphatidylinositol 3-kinase (PI3K)/Akt signaling, which is activated by both liganded IGF1 receptor (IGF1R) and insulin receptor, phosphorylates each of the Foxo proteins at three different Ser/Thr residues (17). The phosphorylated Foxo proteins become inactive and are exported from the nucleus. Subsequently, they become sequestered in the cytoplasm, where they interact with 14-3-3 protein.

In this study, we observe that Foxo1, which is endogenously expressed in PC cells, can interact with AR via the C terminus of the receptor in a ligand-dependent manner and suppress ligand-induced AR transactivation. Foxo1 impaired AR signaling by interfering with ligand-induced AR nuclear translocation and subnuclear compartmentalization as well as receptor-target gene promoter interactions. Furthermore, IGF1/insulin-PI3K/Akt pathway-induced phosphorylation of Foxo1 ameliorated the suppression. Intriguingly, liganded AR stimulated IGF1R expression, suggesting the presence of local positive feedback between IGF1 and AR signaling in PC cells.

EXPERIMENTAL PROCEDURES

Materials—The human PC cell lines LNCaP, DU145, ALVA41, and PC3 were maintained as described previously (18). HEK293 and COS7 cells were maintained in Dulbecco's modified Eagle's medium supplemented with 10% fetal bovine serum, 10 units/liter penicillin, and 10 μg/ml streptomycin in 75-cm^2 flasks in a humidified 5% CO_2 incubator at 37 °C. The following items were obtained commercially: 5α-dihydrotestosterone (DHT; Sigma); IGF1 (R&D Systems, Minneapolis, MN), insulin (Sigma); anti-AR N-terminal (N-20) antibody (Santa Cruz Biotechnology, Santa Cruz, CA); anti-FLAG M2 monoclonal antibody; and anti-FKHR (Foxo1) monoclonal antibody (Sigma).

The firefly luciferase reporter plasmids pGL3-MMTV, pPSA-LUC, GRE-Luc, and pERE2-tk109-LUC, as well as expression vectors for human AR (pCMV-hAR), estrogen receptor (ER) (pSG5-Erα and pSG5-Erβ), GRα (pSG5-GRα), PR (pSG5-PRA and pSG5-PRB), an AR-EGFP chimera (pCMV-AR-GFP), and expression vectors for FLAG-mFoxo1 (mouse) and FLAG-mFoxo1-3A (T24A, S253A, and S316A) chimeras were described previously (18–21). Full-length cDNAs encoding wild-type and mutant mFoxo1 were subcloned in-frame into pEYFP-C2 (Clontech) to generate EYFP-Foxo1 fusion vectors.

PRL-SV40, pG5-Luc, pBIND, and act expression vectors were obtained from Promega (Madison, WI). A full-length cDNA encoding human phosphatase and tensin homolog (PTEN) (mutated in multiple advanced cancers 1) (GenBank™ accession number NM_000314) was obtained from OriGene Technologies, Inc. (Rockville, MD). A full-length cDNA encoding wild-type mFoxo1 was inserted in-frame into the act vector to generate a pACT-Foxo1 chimera. Expression vectors for pBIND-AR-N-(1–660) and pBIND-AR-C-(615–919) chimeras were constructed previously (18).

Relative Luciferase Reporter Assays and Transfection—Relative luciferase reporter assays were performed as described previously (22). Transfections were carried out using FuGENE 6 or FuGENE HD (Roche Applied Science). Stable clones expressing modest amounts of FLAG-Foxo1 or FLAG were established using 600 μg/ml G418 sulfate.

Cell Proliferation Assays—The proliferation of LNCaP cells stably expressing either FLAG-Foxo1 or the control FLAG tag was determined using a CellTiter 96® nonradioactive cell proliferation assay kit (Promega) according to the manufacturer's instructions.

Coimmunoprecipitation, Western Blotting, Mammalian Two-hybrid Assays, and Modified Mammalian One-hybrid Assays—Coimmunoprecipitation, Western blotting, mammalian two-hybrid assays, and modified mammalian one-hybrid assays were performed essentially as described previously (23).

Living Cell Laser Confocal Fluorescence Microscopy Assays—Living cell laser confocal fluorescence microscopy assays were performed essentially as described previously (22). Colocalization and line scan analyses were carried out using the LSM software (version 3.0).

Chromatin Immunoprecipitation (ChIP) Assays—ChIP assays were performed essentially as described previously (24). An anti-AR N-20 antibody and anti-FLAG M2 monoclonal antibodies were applied. Primer information is available upon request.

Real Time PCR—Various transcripts in proper medium-treated cells were analyzed by real time PCR using a LightCycler as described previously (25, 26). Primer information for each target transcript is available upon request.

PSA Measurements—Secretion of human PSA protein into the cell culture medium was measured using an enzyme immunoassay (EIA) at SRL Inc. (Tokyo, Japan).

Statistical Analysis—Data were expressed as means ± S.D. and evaluated by Student's two-tailed t test or ANOVA, followed by post hoc comparisons with Fisher's protected least significant difference test. Values of $p < 0.05$ were considered statistically significant.

RESULTS

Foxo1 Represses Ligand-induced AR Transactivation and Delays LNCaP Cell Proliferation—Initially, the effects of Foxo1 on the transactivation induced by ligand-bound AR were investigated using relative luciferase activity assays. COS7 cells were cotransfected with pCMV-hAR and an artificial luciferase reporter for AR (pGL3-MMTV) together with increasing doses of a Foxo1 expression vector. As shown in Fig. 1*a*, Foxo1 inhibited agonist-induced transcription from the MMTV promoter in a dose-dependent manner. Similarly, the transactivation of endogenous AR monitored by the MMTV promoter in LNCaP human PC cells was suppressed by Foxo1 in a dose-dependent manner (supplemental Fig. 1*a*). Foxo1 also inhibited liganded AR-mediated expression of the promoter of a native AR target gene, *PSA*, in both COS7 (supplemental Fig. 1*b*) and DU145 (supplemental Fig. 1*c*) human PC cells. Thus, the inhibitory effect of Foxo1 on AR, either exogenous or endogenous, is not limited to one cell line and/or promoter. Endogenous Foxo1 mRNA was readily detectable by RT-PCR in all four PC cell

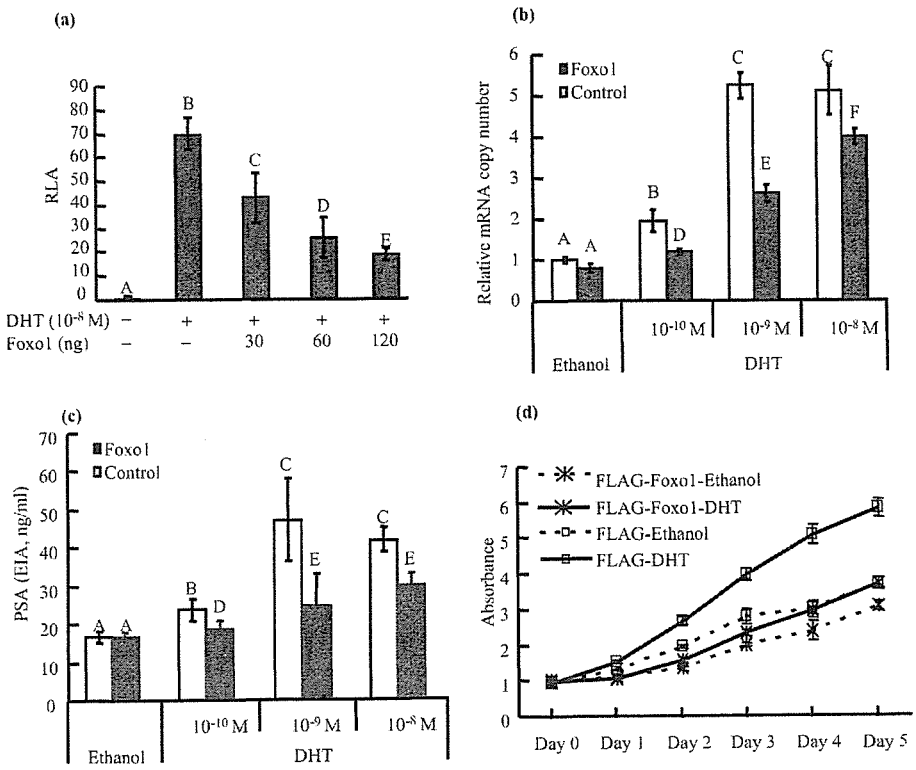

FIGURE 1. **Foxo1 represses ligand-induced AR transactivation and delays LNCaP cell proliferation.** *a*, COS7 cells growing in 24-well plates were transiently cotransfected with a DNA mixture consisting of 300 ng of pGL3-MMTV, 5 ng of pRL-CMV, 30 ng of pCMV-hAR, and increasing amounts (0–120 ng/ml) of FLAG-Foxo1. The empty pcDNA-FLAG vector was cotransfected to equalize the total amount of DNA (in terms of the molar amount) and control for artifacts of the vector DNA. The cells were then treated with 10^{-8} M DHT or the solvent (ethanol) dissolved in serum-free medium for 24 h, before being analyzed by luciferase assays. *b* and *c*, LNCaP cells stably expressing FLAG-Foxo1 or the control FLAG tag were exposed to increasing concentrations of DHT as indicated. Endogenous expression of PSA mRNA (*b*) and PSA protein secreted into the culture medium (*c*) were assayed by real time PCR and EIA, respectively. *d*, LNCaP cells stably expressing either FLAG-Foxo1 or the control FLAG tag were grown in the presence of 10^{-8} M DHT or the solvent (ethanol), and cell proliferation was dynamically evaluated using a CellTiter 96® nonradioactive cell proliferation assay kit. Data are presented as the mean ± S.D. (*a*, *c*, and *d*) or mean ± S.E. (*b*). *Letters above the bars* show statistical groups (ANOVA, $p < 0.05$). *RLA*, relative luciferase activity.

LNCaP cells are typical androgen-responsive PC cells, and their proliferation is largely dependent on the availability of androgen as well as functional AR. To study the effects of Foxo1 on LNCaP cell growth, the two cell lines stably expressing either FLAG-Foxo1 or the control FLAG tag were grown in medium containing charcoal-stripped serum supplemented with either DHT (10^{-8} M) or vehicle (ethanol), and a time course experiment was performed. Among the cells grown in the presence of DHT, the number of FLAG-Foxo1-expressing cells was decreased compared with control cells, even after 1 day of treatment, and then continued to decrease in a time-dependent manner (Fig. 1*d*). The basal proliferation in the presence of ethanol was also reduced to some extent in the stable FLAG-Foxo1-expressing cells, but more prominent inhibition was observed in cells treated with DHT. Thus, Foxo1 overexpression reduced the proliferation of LNCaP cells.

IGF1 Ameliorates Foxo1 Suppression over AR Transactivation—Foxo1 protein is a target of Akt kinase and negatively regulated by phosphorylation in an insulin- and/or IGF1-dependent manner, with resultant nuclear exportation and cytoplasmic sequestration. Therefore, either IGF1 or insulin is expected to attenuate the inhibitory effects of Foxo1 on AR. Initially, we observed that a constitutively active mutant, Foxo1-3A (nonphosphorylatable mutant with all three Akt target residues mutated to alanine, specifically T24A, S253A, and S316A), was more potent than Foxo1 at suppressing DHT-induced AR transactivation (Fig. 2) in LNCaP cells, in which the impaired PI3K/Akt signaling was rescued by cotransfection of PTEN (LNCaP cells lack functional PTEN, and their Akt is constitutively active (27, 28)). In these PTEN-expressing LNCaP cells, IGF1 significantly augmented liganded AR-mediated PSA promoter activities. Of importance, the IGF1-augmented DHT-induced AR transactivation was sharply suppressed by Foxo1-3A but not by wild-type Foxo1. In other words, IGF1 abolished the suppression of liganded AR by wild-type Foxo1 but not that mediated by the Akt-nonphosphorylatable Foxo1 mutant. The rescue by IGF1 was dose-dependent (supplemental Fig. 3*a*) and also found in DU145 cells, which contain intact PTEN and PI3K/Akt signaling (supplemental Fig. 3*c*). Intriguingly, insulin, another PI3K/Akt stimulator, also enhanced the DHT-induced AR transactivation in the PTEN-expressing

lines, namely ALVA41, DU145, LNCaP, and PC3 cells, with DU145 and LNCaP cells showing 2-fold higher expression levels than PC3 and ALVA41 cells (supplemental Fig. 1*d*).

To further explore the relevance of the inhibitory effects of Foxo1 on AR observed in the promoter assays, the androgen-mediated endogenous PSA expression levels were studied in LNCaP cells stably expressing either FLAG-Foxo1 or the control FLAG tag. As shown in Fig. 1, *b* and *c*, DHT-stimulated PSA expression, which was dose-dependent in terms of both the mRNA level (assayed by real time PCR) and the amount of protein secreted into the medium (quantified by EIA), was significantly lower in cells overexpressing Foxo1, indicating that Foxo1 down-regulates the expressions of endogenous androgen-responsive genes. Lentivirus was applied as an additional method for overexpressing Foxo1 in LNCaP cells, and similar results were obtained (supplemental Fig. 1*e*).

Foxo1 also acted on other steroid hormone receptors (supplemental Fig. 2). Specifically, it enhanced the transcription mediated by liganded PR-A, PR-B, and GRα, exhibited no dramatic effect on ERα, but suppressed ERβ function in a similar manner to that observed for AR. Thus, the inhibitory effects are relatively specific for AR and ERβ.

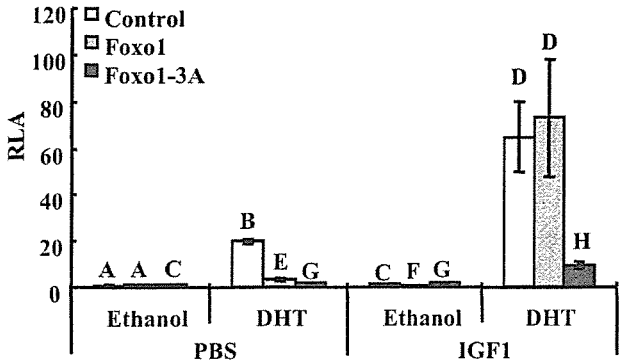

FIGURE 2. **IGF1 ameliorates Foxo1-suppressed AR transactivation.** LNCaP cells growing in 24-well plates were cotransfected with 100 ng of FLAG-Foxo1, FLAG-Foxo1-3A (Akt-nonphosphorylatable constitutively active mutant), or an equimolar amount of pcDNA-FLAG together with 400 ng of PSA-Luc, 5 ng of pRL-CMV, 40 ng of PTEN, and 40 ng of pCMV-hAR. At 48 h post-transfection, the cells were exposed to 10^{-8} M DHT and/or 100 ng/ml IGF1 in serum-free medium for 24 h, before being lysed and analyzed by luciferase assays. *Letters above the bars* show statistical groups (ANOVA, $p < 0.05$). The ascending order of the groups is as follows: F, A, C, G, E, H, B, and D. *RLA*, relative luciferase activity.

LNCaP cells in a concentration-dependent manner, albeit less potently (supplemental Fig. 3*b*).

To exclude the possibility that Foxo1 inhibits AR transactivation by decreasing the protein level of the receptor, the AR protein level was examined by immunoblotting under the same conditions used for the reporter assays. As shown in supplemental Fig. 4, *a–c*, cotransfection of Foxo1 with AR into LNCaP cells did not alter the AR protein level in either the presence or absence of DHT. Similarly, the AR mRNA expression level in lentiviral Foxo1-infected LNCaP cells was not significantly altered (supplemental Fig. 4*d*). Hence, these data indicate that Foxo1 suppresses the specific activity of the receptor.

Physical Interaction between Foxo1 and AR—Next, we examined whether there is a direct physical interaction between AR and Foxo1 by using coimmunoprecipitation assays. LNCaP cells cotransfected with FLAG-Foxo1 and pCMV-hAR together with PTEN and grown in serum-free medium were treated with IGF1, insulin, or PBS in combination with DHT or ethanol. As shown in Fig. 3*a* (*upper panel*), FLAG-Foxo1 bands were detected in anti-AR antibody-precipitated immune complexes from cells treated with DHT (*lanes 6–8*), whereas a very weak signal was detected in ethanol-treated cells (*lane 2*), suggesting that Foxo1 and AR interact directly, and their interaction is significantly enhanced by the AR ligand. The presence of IGF1 or insulin did not abolish the interaction (Fig. 3*a* (*upper panel*), *lanes 7* and *8*), although both molecules appeared to reduce the amount of Foxo1 protein interacting with liganded AR. In contrast, no Foxo1 signal was detectable in normal rabbit IgG-precipitated immune complexes from cells treated with either ethanol (Fig. 3*a* (*upper panel*), *lane 1*) or DHT (*lane 5*), indicating the specificity of the Foxo1-AR interaction. Using PTEN-expressing LNCaP cells, we further verified that endogenous AR and Foxo1 interacted in an androgen-dependent manner (supplemental Fig. 5), suggesting that the observed interaction is physiologically meaningful and that Foxo1 may repress liganded activated AR via a direct protein-protein interaction.

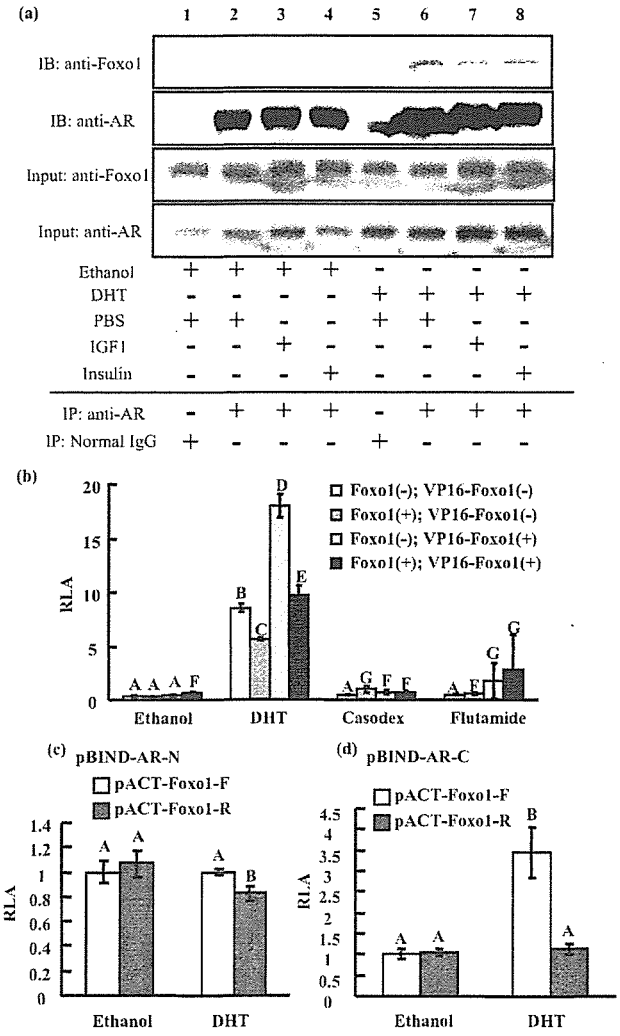

FIGURE 3. **Physical interaction between Foxo1 and AR.** *a*, coimmunoprecipitation of AR with Foxo1. LNCaP cells transfected with PTEN, pCMV-hAR, and pcDNA-FLAG-Foxo1 or the control empty vector pcDNA-FLAG were treated with PBS, IGF1 (100 ng/ml), or insulin (10 μg/ml) in combination with DHT (10^{-8} M) or ethanol as indicated. Aliquots (1000 μg) of whole cell extracts were incubated with 5 μg of rabbit anti-AR (N-20) antibody or control normal rabbit IgG together with 50 μl of protein A beads, and the presence of FLAG-Foxo1 in the immunoprecipitates (*IP*) was detected by immunoblotting (*IB*) with an anti-Foxo1 mouse monoclonal antibody. Immunoprecipitation of AR by the anti-AR (N-20) antibody was validated by using an anti-AR antibody obtained from Cell Signaling (catalog number 3202). The presence of AR and Foxo1 in the input cell lysate samples were confirmed. *b*, modified one-hybrid assays. COS7 cells were cotransfected with 50 ng of vectors for Foxo1 (pcDNA-FLAG-Foxo1), VP16-Foxo1 fusion protein (pACT-Foxo1), or both together with 300 ng of pGL3-MMTV, 5 ng of pRL-CMV, and 50 ng of pCMV-hAR and subsequently treated with 10^{-8} M DHT, 10^{-6} M casodex, 10^{-6} M hydroxyflutamide, or the solvent (ethanol), respectively, for 24 h, before being analyzed by luciferase assays. Note that the DHT-induced AR transactivation is inhibited by Foxo1 but enhanced by VP16-Foxo1. The ascending order of the groups is A, F, G, C, B, E, and D. *c* and *d*, the C terminus of AR mediates the interaction with Foxo1. Mammalian two-hybrid assays were carried out to test for an *in vivo* interaction between AR and Foxo1. COS7 cells were cotransfected with a DNA mixture consisting of 100 ng of pG5-LUC, 1.5 ng of pRL-CMV, and 75 ng of pACT-Foxo1 together with 25 ng of pBIND-AR-N (*c*) or equimolar amounts of pBIND-AR-C (*d*). After the transfection, the cells were treated with 10^{-8} M DHT or ethanol. Parallel experiments in which pACT-Foxo1 was replaced with pACT-Foxo1-R (Foxo1 fused with VP16 in the reverse orientation) were carried out as controls. *Letters above the bars* show statistical groups (ANOVA, $p < 0.05$). *RLA*, relative luciferase activity.

The interaction was further confirmed by modified mammalian one-hybrid assays (29). COS7 cells were cotransfected with an MMTV reporter and AR together with wild-type Foxo1,

pACT-Foxo1, or both, and then treated with DHT or two antiandrogens, namely hydroxyflutamide and casodex. As shown in Fig. 3*b*, FLAG-Foxo1 inhibited DHT-induced AR transactivation as expected. However, pACT-Foxo1 (with a viral VP16 activation domain fused to the Foxo1 N terminus) enhanced the liganded AR function, and the coexistence of FLAG-Foxo1 and pACT-Foxo1 neutralized the luciferase activity. Thus, although Foxo1 was suppressive toward AR, VP16-Foxo1 became an artificial coactivator for AR, and this remarkable shift strongly suggests that there is a direct interaction between AR and Foxo1. Interestingly, the antiandrogens casodex and hydroxyflutamide did not produce the same phenomenon, suggesting that only an agonist can induce the interaction.

Further clarification of the individual domains of AR responsible for the interaction with Foxo1 was carried out by mammalian two-hybrid assays, in which the AR N terminus (amino acids 1–660) and C terminus (amino acids 615–919) were individually fused to the DNA-binding domain of GAL4 to produce pBIND-AR-N and pBIND-AR-C, respectively. As a control, the full-length Foxo1 cDNA was fused to the VP16 activation domain in either the forward (pACT-Foxo1-F) or reverse orientation (pACT-Foxo1-R). In comparison with pACT-Foxo1-R, pACT-Foxo1-F did not alter the activity of the pG5-LUC reporter coexpression with pBIND-AR-N in either the presence or absence of the ligand, suggesting a lack of interaction between the AR N terminus and Foxo1 (Fig. 3*c*). In the case of pBIND-AR-C coexpression, pACT-Foxo1-F, but not pACT-Foxo1-R, significantly stimulated the reporter in the presence of DHT (Fig. 3*d*). These data indicate that the AR C terminus interacts with Foxo1 in a hormone-dependent manner.

Subcellular Interactions between Foxo1 and AR in Living Cells—The intracellular distribution of EYFP-Foxo1 in living COS7 cells was visualized using laser confocal scanning microscopy. Consistent with previous observations (17), EYFP-Foxo1 in serum-starved COS7 cells was predominantly located in the nucleus in a homogeneous manner, with relatively weak diffuse fluorescence also visible in the cytoplasm (Fig. 4*a*). However, the nuclear accumulation of Foxo1 varied among the examined cells (supplemental Fig. 6, *a–c*). This variation was presumably because of differing IGF1/insulin signaling tones among the different cells, because challenge with IGF1 caused 100% of the EYFP-Foxo1-expressing cells to show complete cytoplasmic fluorescence (Fig. 4*b*). As expected, EGFP-AR predominantly showed diffuse fluorescence in the cytosol with very weak nuclear fluorescence in the absence of the ligand (Fig. 4*c*), whereas DHT induced complete nuclear translocation and typical subnuclear foci formation (Fig. 4*d*). When EYFP-Foxo1 and EGFP-AR were coexpressed, both proteins showed their original distribution patterns in cells treated with the control solvents (IGF1−/DHT−; Fig. 4*f*). Among the cells treated with DHT alone (IGF1−/DHT−; Fig. 4*g*), the distribution of EYFP-Foxo1 remained almost unchanged, whereas EGFP-AR exhibited incomplete nuclear translocation and significantly impaired subnuclear compartmentalization (foci formation) and was diffuse in both the nucleus and cytoplasm. Although a subgroup of cells showed relatively complete nuclear translocation, their foci formation was apparently impaired (supplemental Fig. 6*d*). In cells treated with IGF1 alone (IGF1+/DHT−; Fig. 4*i*), EYFP-Foxo1 was completely exported to the cytoplasm, whereas EGFP-AR maintained its original distribution, namely predominant diffuse cytoplasmic localization with weak nuclear fluorescence. In comparison with IGF1−/DHT+ cells (Fig. 4*g*), EGFP-AR in cells treated with both ligands (IGF1+/DHT+; Fig. 4*j*) showed more complete nuclear translocation and, importantly, also exhibited significantly improved subnuclear compartmentalization.

To quantitatively evaluate the effects of IGF1/Foxo1 on the subnuclear distribution of liganded AR, the intranuclear distribution patterns of EGFP-AR in the cell populations, shown representatively in Fig. 4, *d*, *g*, and *j*, were subjected to line scan analyses using the LSM software as described previously (22). In Fig. 4, *e*, *h*, and *k* show the line scan data of *d*, *g*, and *j*, respectively. In total, 20 cells from each group were subjected to the line scan analyses. The fluorescence intensity of the cells in Fig. 4*d* was quite heterogeneous (heterogeneity index (HI) = 53.12 ± 10.53), whereas cotransfection of Foxo1 (*cells* in Fig. 4*g*) decreased the HI to 17.83 ± 9.46, indicating that the AR distribution in these cells was quite constant. The HI value recovered to 35.16 ± 18.89 in cells further treated with IGF1 (*cells* in Fig. 4*j*), suggesting that the Foxo1-inhibited subnuclear reorganization of liganded AR was partially rescued by IGF1.

3T3-L1 cells contain a relatively high quantity of endogenous AR, which undergoes typical subnuclear reorganization and forms fine foci in the presence of DHT (23). To address whether Foxo1 also suppresses the foci formation of endogenous AR, EYFP-Foxo1 was expressed in 3T3-L1 cells, and the endogenous AR distributions in the presence and absence of DHT were studied by immunofluorescence staining. As shown in supplemental Fig. 7, DHT-induced AR foci were significantly suppressed by Foxo1 overexpression. Specifically, the HI of liganded nuclear AR was 66.26 ± 15.77 ($n = 20$) in the absence of Foxo1 but reduced to 38.25 ± 8.91 ($n = 20$, $p < 0.01$) by Foxo1.

The distribution of EYFP-Foxo1 in cells coexpressing EGFP-AR and treated with both ligands (IGF1+/DHT+) was striking in that a substantial amount of Foxo1 remained in the nucleus (Fig. 4*j* and supplemental Fig. 6*e*). This distribution is in great contrast to that in the cells in Fig. 4, *b* and *i*, where IGF1 induced complete nuclear export of Foxo1 in all cells. These observations suggest that liganded AR sequestered part of the Foxo1 in the nucleus, even in the presence of IGF1. Furthermore, the nuclear Foxo1 in these cells was heterogeneous and colocalized with ligand-bound AR (Fig. 4*j* and supplemental Fig. 6*e*), suggesting an interaction between the two proteins.

In contrast to EYFP-Foxo1, EYFP-Foxo1-3A resided in the nucleus in a reticular manner regardless of the IGF1 availability. Furthermore, it disrupted DHT-induced AR foci formation, and importantly, the disruption was not rescued by IGF1 (supplemental Fig. 8).

Interaction of Foxo1 and AR within the Human PSA Promoter—Next, ChIP assays were carried out to determine whether Foxo1 and AR associate with the chromatin of an AR target gene promoter *in vivo*. LNCaP cells cotransfected with pcDNA-FLAG-Foxo1 and pCMV-hAR were subjected to serum starvation and challenged with IGF1, insulin, or PBS as a control in the presence of DHT or the solvent (ethanol).

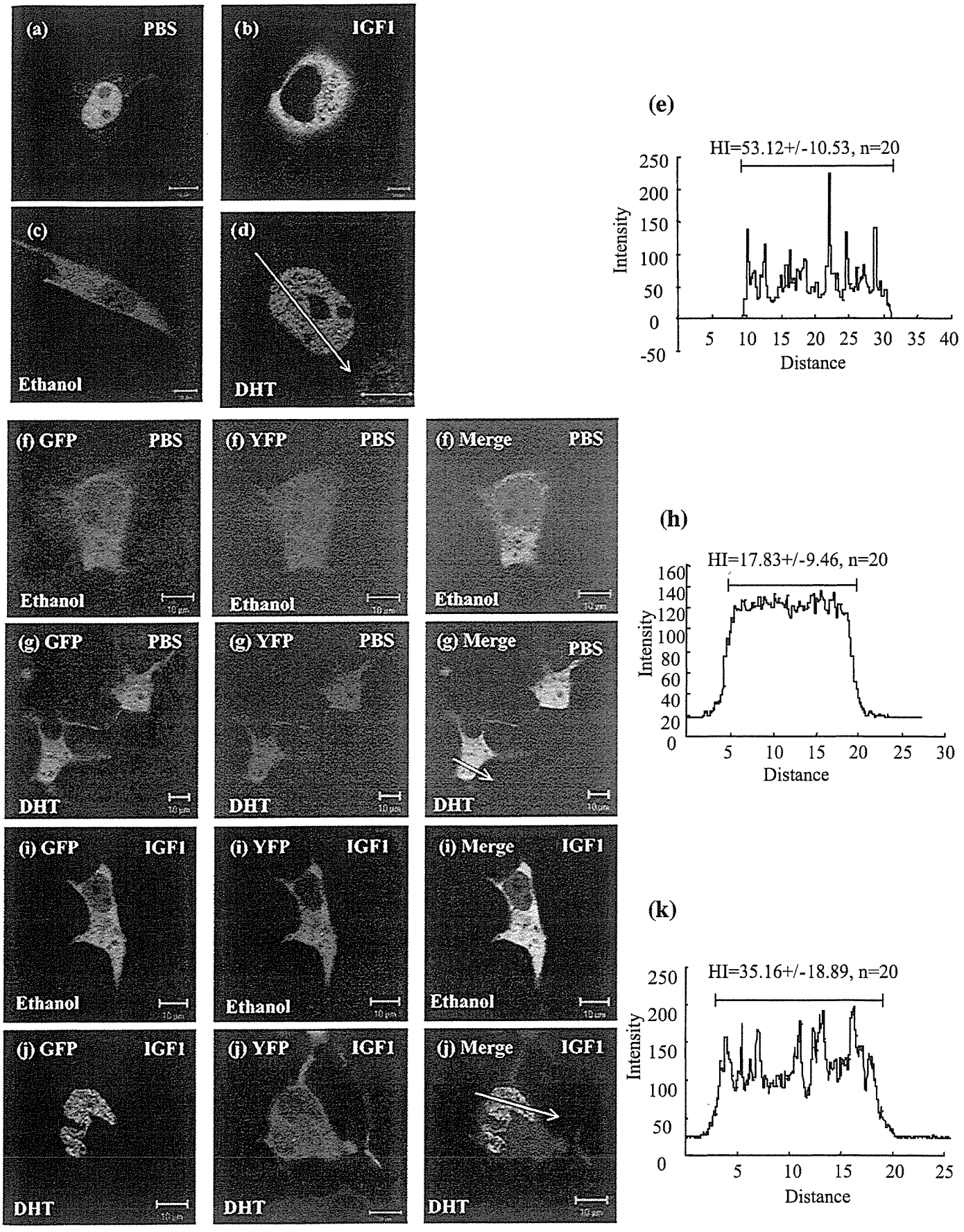
(a) PBS
(b) IGF1
(c) Ethanol
(d) DHT
(e)
HI=53.12+/-10.53, n=20
Intensity
Distance
(f) GFP PBS
(f) YFP PBS
(f) Merge PBS
Ethanol
(g) GFP PBS
(g) YFP PBS
(g) Merge PBS
DHT
(h)
HI=17.83+/-9.46, n=20
Intensity
Distance
(i) GFP IGF1
(i) YFP IGF1
(i) Merge IGF1
Ethanol
(j) GFP IGF1
(j) YFP IGF1
(j) Merge IGF1
DHT
(k)
HI=35.16+/-18.89, n=20
Intensity
Distance

Genomic DNA corresponding to the androgen-response elements ARE I/II and ARE III, which are located in the promoter and enhancer of the *PSA* gene, respectively, was remarkably enriched in a DHT-dependent manner, as evaluated using an anti-FLAG antibody (Fig. 5*b*). Weak bands were detectable in the absence of any ligand, whereas treatment of the cells with IGF1 or insulin either abolished or significantly reduced the occupancy of the DNA by Foxo1, regardless of the presence or absence of DHT. There was very weak Foxo1 occupancy of the DNA in a region between the enhancer and the promoter, but no enrichment was detected in the presence of DHT, thus demonstrating specificity (Fig. 5*b*). Again, the weak bands vanished in the presence of IGF1 or insulin. The association of Foxo1 with the chromatinized *PSA* promoter was specific, because DNA from the *GAPDH* gene was not precipitated (Fig. 5*b*). Thus, agonist-bound AR induces specific associations of Foxo1 with chromatin AREs on the *PSA* promoter, demonstrating that Foxo1 and AR form a ligand-dependent complex on chromatin. Furthermore, IGF1 and insulin are able to remove Foxo1 from chromatinized DNA.

The ChIP assays further revealed that Foxo1 interfered with ligand-induced recruitment of AR to the *PSA* promoter in LNCaP cells. The cells were transfected with pCMV-hAR together with pcDNA-FLAG-Foxo1-3A or pcDNA-FLAG and treated with the ligand as described above. Chromatin-transcription factor complexes were precipitated with an anti-AR antibody and combined with real time PCR analysis to quantify the relative number of immunoprecipitated DNA copies to the input control for each sample as described previously (24). Small amounts of the DNA segments corresponding to *PSA* ARE I/II and ARE III were detected in the absence of DHT, and DHT induced significant enrichment of these amounts (Fig. 5*c*). IGF1 or insulin increased the AR-DNA interaction under each circumstance (presence or absence of DHT; Fig. 5*c*). Overexpression of the nonphosphorylatable Foxo1-3A significantly reduced the relative copy numbers of *PSA* promoter DNA at both positions, especially in the presence of DHT (Fig. 5*c*), suggesting that the association between the *PSA* promoter and liganded AR was impaired. Furthermore, Foxo1-3A also substantially abolished the responsiveness to IGF1 and insulin (Fig. 5*c*), indicating that intact and phosphorylatable Foxo1 is vital for IGF1 or insulin to enhance the liganded AR-DNA interaction.

Activation of AR Stimulates IGF1R Expression in LNCaP Cells—We further found that IGF1R expression was up-regulated in LNCaP cells in the presence of DHT. As shown in Fig. 6*a*, DHT treatment for 24 h dose-dependently increased the IGF1R mRNA levels in serum-starved LNCaP cells, and 10^{-8} M DHT boosted the mRNA level by 17-fold. This stimulation of IGF1R was relatively specific, because comparable concentrations of DHT did not increase the levels of epidermal growth factor receptor (supplemental Fig. 9*a*) and Foxo1 mRNAs (supplemental Fig. 9*b*). An autoregulation process may occur, because the up-regulated IGF1R is expected to enhance IGF1-PI3K-Akt signaling, thereby resulting in a further gain-of-function of AR via phosphorylation of the repressive Foxo1.

DISCUSSION

Foxo1 Suppression and IGF1-related Mechanism of Refractory PC—IGF1 is capable of reactivating AR in low or absent androgen environments and therefore represents one of the suggested multiple mechanisms by which PC cells progress to the androgen-insensitive stage (7). However, the mechanisms by which IGF1 and other growth factors regulate AR-mediated transcription in PC cells remain unclear.

IGF1, via binding to its receptor IGF1R, activates intracellular signaling pathways that favor proliferation and cell survival. One of the most important pathways that becomes activated is the PI3K/Akt pathway (30), because activation of this pathway by IGF1, as well as other molecules, has been implicated in PC. Specifically, increases in IGF1R expression (11, 31, 32) and loss of the tumor suppressor gene *PTEN* (27, 28) elicit increased activity of the PI3K/Akt pathway and greatly contribute to tumor progression of PC.

Foxo1, which is endogenously expressed in PC cells, is functionally inhibited by phosphorylation at Ser-253, Ser-316, and Thr-(24 in response to IGF1 or insulin through PI3K/Akt kinase (17). Overexpression of Foxo1 in PC cells leads to apoptosis (33). Our present results have revealed that Foxo1 directly interacts with and suppresses the transactivation of AR, whereas IGF1 signaling ameliorates this suppression and results in AR gain-of-function. Thus, considering the reported mechanism that β-catenin may mediate the stimulatory effect of IGF1 signaling on AR (34), Foxo1 may represent an alternative explanation.

Because insulin induces PI3K-Akt signaling and the resultant modification of Foxo1 (17), similar to IGF1, and also enhances AR transactivation in PTEN-expressing LNCaP cells, it is of great value to further elucidate whether insulin signaling enhances AR function via a similar mechanism. Regarding this point, it is noteworthy that the syndrome of insulin resistance, which is characterized by an increased insulin level and abdom-

FIGURE 4. **Subcellular interaction between Foxo1 and AR in living COS7 cells.** The expressions of chimeric fluorescent proteins were observed in living COS7 cells using a Zeiss LSM 510 META laser confocal microscope as described under "Experimental Procedures." *a* and *b*, COS7 cells were transfected with 0.5 μg/dish of EYFP-Foxo1 and then treated with PBS (*a*) or 100 ng/ml IGF1 (*b*). *c* and *d*, COS7 cells expressing EGFP-AR were exposed to ethanol (*c*) or 10^{-8} M DHT (*d*), respectively. *f*, *g*, *i*, and *j*, COS7 cells coexpressing EGFP-AR and EYFP-Foxo1 were exposed to DHT and/or IGF1 as indicated in the individual panels. The fluorescence signals for green fluorescent protein (*GFP*) and yellow fluorescent protein (*YFP*) and the merged images are shown separately. *e*, *h*, and *k*, line scan analyses. A *straight line* was drawn through the target cell, and the fluorescence intensities along the line were recorded. The mean and S.D. values of the fluorescence intensity signals for the segment of interest (nucleus, avoiding the nucleoli) were calculated. The heterogeneity of the fluorescence intensity along the segment of interest was evaluated by the parameter of the HI, which was calculated using the following formula: HI = 100 × S.D./mean. A fluorescence intensity fluctuation graph, which clearly demonstrated the heterogeneity, was then created by plotting the intensity against the distance along the line. The lines obtained by line scan analyses are shown for representative cells. The fluorescence intensity fluctuation graphs of the representative cells are shown in *e*, *h*, and *k* and relate to the cells in *d*, *g*, and *j*, respectively. The *x* axis represents the distance along each line, whereas the *y* axis shows the fluorescence intensity. The *bar* within each graph marks the segment of the line for which the HI analysis was performed, and the corresponding intensity and HI values are indicated at the *top* of each graph. *Scale bars*, 10 μm.